IEEE Access
Multidisciplinary ⋮ Rapid Review ⋮ Open Access Journal

Received 13 January 2023, accepted 5 February 2023, date of publication 9 February 2023, date of current version 14 February 2023.

Digital Object Identifier 10.1109/ACCESS.2023.3243800

TOPICAL REVIEW

A Review on Vanadium Redox Flow Battery Storage Systems for Large-Scale Power Systems Application

ANUOLUWAPO ALUKO, (Member, IEEE), AND ANDY KNIGHT, (Senior Member, IEEE)
Power Research Laboratory, Department of Electrical and Software Engineering, University of Calgary, Calgary, AB T2N 1N4, Canada
Corresponding author: Anuoluwapo Aluko (anuoluwapo.aluko@ucalgary.ca)

This work was supported by the Power Research Laboratory, University of Calgary.

ABSTRACT In the wake of increasing the share of renewable energy-based generation systems in the power mix and reducing the risk of global environmental harm caused by fossil-based generation systems, energy storage system application has become a crucial player to offset the intermittence and instability associated with renewable energy systems. Due to the capability to store large amounts of energy in an efficient way, redox flow batteries (RFBs) are becoming the energy storage of choice for large-scale applications. Vanadium-based RFBs (V-RFBs) are one of the upcoming energy storage technologies that are being considered for large-scale implementations because of their several advantages such as zero cross-contamination, scalability, flexibility, long life cycle, and non-toxic operating condition. This review presents the current state of the V-RFB technology for power system applications. The basic working operation of the V-RFB system with the principle of operation of its major components, the design considerations, and the limitations of each component are discussed. It presents technical information to improve the overall performance of the V-RFB by considering the materials of the cell components, modeling methods, stack design, flow rate optimization, and shunt current reduction.

INDEX TERMS Energy storage system, flow battery, renewable energy, vanadium redox flow battery.

I. INTRODUCTION

In recent years, the energy sector has accounted for about 75% of the total emissions that have increased the world's temperature by 1.1°C with noticeable weather and climate changes [1]. In spite of this, energy is still important in livelihoods and in the continuous growth in the human population that pushes the demand for energy services to higher scales. To meet the increasing demand for energy and reduce the emissions from conventional energy sources that dominate the power grid, renewable energy (RE) sources have begun to play important roles [2], [3]. Notwithstanding the effect of COVID-19 lockdowns on the global economy, RE sources like solar and wind have kept on growing at an exponential rate to meet the increasing energy demands with their clean energy characteristics. In several countries, solar and wind energy are the cheapest source of energy for the generation of electricity [1].

While there is a global consensus that large-scale utilization of RE sources is required for sustainable development, their intermittence and uncontrollable nature make it difficult to directly integrate them into the grid. Therefore, methods to improve the quality and reliability of supply must be introduced. One of the methods to increase the penetration level of large-scale RE sources into the grid is the application of energy storage systems (ESS) [4], [5], [6]. ESS is beneficial to maintain the balance between generation and demand in a high RE-dominated grid, thereby maintaining or improving the stability and resilience of the grid. In off-peak periods, ESS can store excess energy from the RE source and release the energy during peak periods. In large power grids, ESS plays a crucial role in increasing the penetration of RE, smoothing the power output from RE sources, increasing the operating reserve, reducing peak load

The associate editor coordinating the review of this manuscript and approving it for publication was Jiefeng Hu.

regulation capacity of the grid, and providing ancillary services such as frequency regulation, low voltage ride-though, reactive power support, fluctuation suppression, black start capability, etc. [7], [8], [9], [10], [11]. In developing an appropriate energy storage technique for large-scale application, characteristics such as scalability, high storage capacity, quick response time, high efficiency, long life cycle, low environmental impacts, and low cost must be considered [12], [13], [14], [15], [16]. Several energy storage techniques have been developed for various applications. They are generally grouped into chemical, electrical, mechanical, and thermal ESS technologies; Table 1 shows the widely used ESS technologies with their respective advantages and disadvantages. Presently, no single ESS technology meets all the satisfactory requirements for large-scale applications [17]. For example, pumped hydro-ESS and compressed air-ESS that have mature technology are limited by site locations and other environmental safety factors [18], [19]. Super capacitor-ESS have very fast response times but are limited by their low energy density, high self-discharge losses, and high cost of materials for large-scale applications [20], [21]. Battery-based ESS technologies like Lead-acid and Lithium-ion batteries have the advantages of economies of scale and high energy density but are highly sensitive to operating temperature [22], [23].

With the continuous development in the ESS industry for large-scale applications, redox flow batteries (RFBs) have been recently deployed to meet large-scale ESS requirements. RFB is a type of battery ESS that uses a soluble pair of redox electrolytes in the two half-cells. The electrolyte for each half-cell is stored in an external tank and is pumped into the cell where the electrochemical reactions (redox) occur. The electrolytes in the half-cells are separated by a membrane to avoid a direct mixture of the electrolytes. The major advantage of the RFB is the independence between the energy capacity and power capacity [24]. The energy capacity of the RFB is proportional to the volume and concentration of the electrolytes, and the power of the RFB is dependent on the size of the electrodes and the behavior of the active materials in the cell. This makes the cost of increasing the energy capacity of the RFB marginally decline with increasing the storage capacity. Therefore, the RFB is a flexible and scalable ESS technology [25], [26], [27], [28]. The RFBs have few rotating parts and do not often need the operator's attention, making them have low maintenance and operating costs [29]. Due to the reversibility of the redox reactions in the RFBs, they tend to possess longer life cycles compared to other ESS technologies [30]. They can fully discharge without causing damage to the battery components [31], [32]. For power system applications, RFBs are a good choice because they have fast response times (milliseconds) that are required for power smoothing in intermittent RE-based generations [31]. These beneficial features have increased the research and development of RFB technology for large-scale power systems applications. Contrary to the aforementioned advantages of the RFBs, they are associated with some drawbacks such as low energy density that make them suitable for stationary applications, unlike electric vehicle (EV) applications where size and weight are important factors for usability. Some RFB variants have reactions that may reduce the power capacity and system efficiency. They are associated with parasitic losses that reduce overall efficiency. Another major drawback is the high cost of the materials required to develop RFBs, the majority of the RFB research is centered on developing new materials for the RFB components to reduce its overall cost [33], [34], [35].

With the number of RFB technologies that have been developed in recent years, the Vanadium-based RFB (V-RFB) has received the most attention. The major reason is its benefits over other types of RFBs. V-RFBs adopt a single element (vanadium) with various oxidation states in its electrolytes, therefore, the possibility of cross-contamination is very low [36]. There is a possibility of recycling the electrolytes between applications [37]. V-RFBs have the capability of ion crossover regeneration during regular operation [37]. They have low levels of charge cycles compared to other RFBs [38]. The capacity of the V-RFBs can be recovered because the vanadium ions used in the electrolytes do not degrade, and only the oxidation states change [39]. They are environmentally safe, do not release toxic compounds, and have a low risk of explosion at high temperatures relative to other batteries [39]. Contrariwise to these benefits, the V-RFB has some disadvantages that include low energy/volume ratio, deterioration of membrane and anode terminal due to high oxidation properties of vanadium ions [40], reduced cell efficiency and electrode surface area as a result of side reactions at the electrodes [41], [42], [43].

Given the potential benefits of the V-RFB and the growing demand for large-scale energy storage to expedite the penetration of RE systems, this review encapsulates the current updates of the V-RFB technology based on past and current developments, materials, modeling methods, and the effect of internal parameters on their overall efficiency and performance that are consequential to their large-scale commercialization. Therefore, this review benefits researchers and scientists to understand the requirements of the V-RFBs for large-scale applications; and engineers to understand the limitations and current developments in the V-RFB technology for large-scale applications. Different from the V-RFB reviews that have been reported in the literature, this paper presents a review that covers the physicochemical and electrochemical processes of the V-RFB system including the practical limitations of the V-RFB components that affect its large-scale application, the current projects in the V-RFB industry, cost implications of large-scale V-RFB systems, and practical methods that have been adopted to improve the performance and reduce the overall cost of the V-RFB system for large-scale applications.

The remainder of this article is organized as follows; Section II gives a brief history of the V-RFB development and technology with different projects that have been

TABLE 1. Advantages and disadvantages of different ESS technologies.

S/N	ESS Technology	Advantages	Disadvantages
1	Pumped Hydro	• Mature technology • Long life cycle • High capacity	• Requires specific location • High initial cost • Lengthy construction time • Environmental concerns due to site location
2	Compressed Air	• Mature technology • Long storage period • Low initial cost • High capacity	• Requires appropriate location • Limited flexibility • Limitation of fossil fuel combustion
3	Flywheel	• Low maintenance • Fast charge and discharge cycles • High power density • Long life cycle	• High flywheel requirements • Significant maintenance cost due to high speed of operation • Short storage time • Risk of mechanical failure
4	Super Capacitor	• Fast charging time • Fast response time • High power density • Low maintenance cost	• Low energy density • High self-discharge loss • High cost to develop advanced materials • Needs cooling for effective operation
5	Lead-Acid	• Mature technology • High number of charge/discharge cycles • Fast response time • High recycling potential	• Short life cycle • Susceptible to sulfation • Poor performance at low temperatures • Low energy density at low temperatures
6	Lithium-ion	• High energy density • High power density • Fast response time • Mature technology • Little environmental impact • Not suitable for full-discharge applications	• Short life cycle • Highly sensitive to operating temperatures • Needs internal overcharge protection technology
7	Fuel Cell	• High energy density • Highly scalable • Fast discharging with near-zero self-discharge	• Low life cycle • Low system efficiency • Expensive hardware requirements
8	Superconducting magnetic Energy Storage	• High power density • High efficiency • Low power losses • Long life cycle • Fast response time	• High cost • Low temperature operation that requires a refrigeration system • High self-discharge rate
9	Redox Flow Battery	• High flexibility and scalability • Low environmental impact • Long life cycle • Low maintenance cost • Long discharge duration	• Low energy density • High cost

completed recently, Section III provides details on the operating principles of the V-RFB with developments of the major components of the V-RFB including the performance metrics for V-RFBs, Section IV presents the modeling methods of the

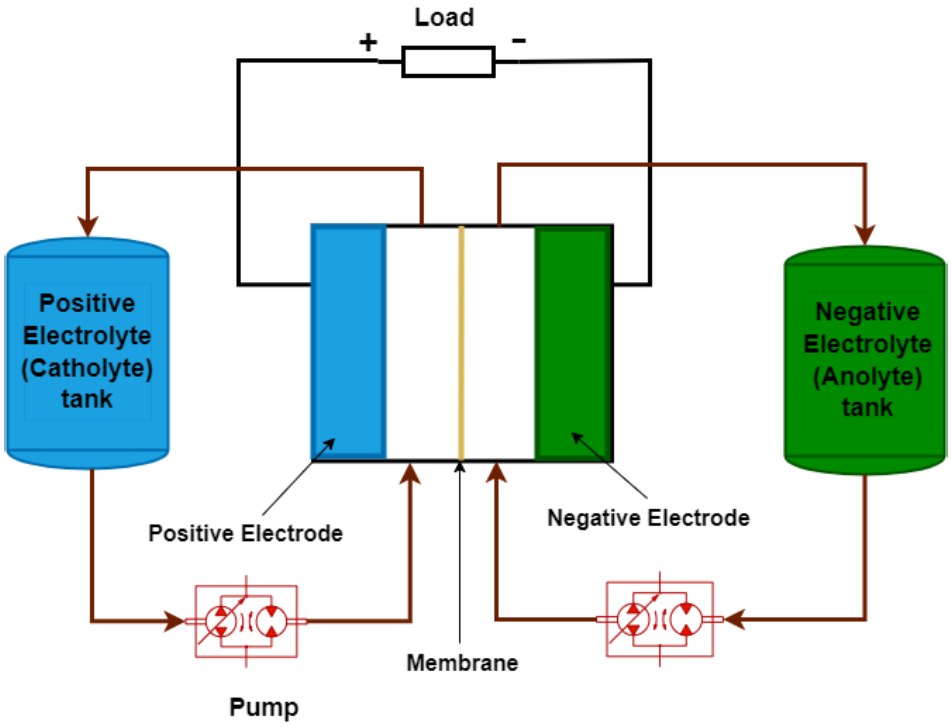

FIGURE 1. Schematic representation of a single cell V-RFB.

V-RFBs, Section V presents the key factors that impact the performance and commercialization of the V-RFB systems for large-scale applications, Section VI discusses the various utilization of the V-RFB in RE-integrated systems, and Section VII concludes the review with research directions for future consideration.

II. BRIEF HISTORY OF REDOX FLOW BATTERIES

The early RFBs were developed by the United States National Aeronautics and Space Administration (NASA) in the 1970s [44]. This RFB system is known as the Iron-chromium battery (ICB) because it used Iron (Fe2+/Fe3+) and Chromium (Cr3+/Cr2+) in the positive electrolyte (catholyte) and negative electrolyte (anolyte) half cells. A single-cell ICB has an open circuit voltage of 1.18 V. The intrinsic drawback of the ICB is the low CE and depth-of-charge due to the low redox potential of the catholyte. The ICB was commercialized for large-scale application by EnerVault, USA and under the Moonlight project in Japan [45]. By replacing the Chromium in ICB with Vanadium, the Pacific Northwest National Laboratory, USA developed the Iron-Vanadium (FeV) RFB. The FeV-RFB has a low cell potential difference (p.d.) of 1.02 V which leads to low energy density that can be bolstered by increasing the concentration of the electrolytes [46], [47]. Large-scale Zinc-Bromine (ZnBr) RFB with a cell p.d. of 1.85 V was developed and commercialized [48]. While the ZnBr-RFB offers high energy density, future developments were thwarted because of the corrosive nature and toxicity of the Bromine vapor [49]. To address the safety concerns of the ZnBr-RFB, the Zinc-Iodine (ZnI) RFB was developed, the trade-off of the ZnI-RFB compared to the ZnBr-RFB is the low cell voltage of 1.30 V [50]. Using Sodium-bromide and sodium-polysulfide in the positive and negative half cells of the electrolyte tanks, the polysulfide-bromine (SpBr) RFB was developed by Innogy, United Kingdom (UK) [51]. The SpBr-RFB has a cell p.d. of 1.35 V with an EE of approximately 65%. The drawbacks of the SpBr-RFB are the sedimentation of sulfur on the membrane which causes electrolytic imbalance and the toxic nature of the bromine emissions. In 2004, the Zinc-Cerium (ZnCe) RFB was developed by Plurion, UK [52]. The ZnCe-RFB system uses Zn2+/Z+ in the negative half cell and Ce3+/Ce4+ in the positive half cell, having an open circuit cell voltage of 2.43 V. Based on the report in [53], the large-scale application of the ZnCe-RFb has been unsuccessful. Another Zinc-based RFB system that has been developed is the Zinc-Nickel (ZnNi) RFB. The single cell ZnNi-RFB has a p.d. of 1.7 V with a CE of 96%. Compared to other Zinc-based RFBs, the ZnNi is the least expensive with a low propensity to emit toxic gases. In 2013, the ZnNi-RFB was commercialized for microgrid applications by ViZn Energy System, USA [54]. It is worth mentioning that the RFB systems presented so far use different redox pairs for their redox reactions, i.e., the element of the electrolyte in the positive half-cell is different from the element of the electrolyte in the negative half-cell.

This feature leads to cross-contamination or diffusion in the RFB system which leads to capacity decay, the decline in the battery overall efficiency, and is unsuitable for long-term large-scale applications. These limitations have led to the development of single-element RFB systems.

Due to the availability and low cost of Iron, the all-Iron RFB that utilizes Fe2+ in both half cells of the RFB was developed and patented by Savinell and his team [52], [65]. While the all-Iron has received considerable research attention, it has the limitation of low power density and overall system efficiency [66]. The University of New South Wales (UNSW) Professor Maria Skyllas-Kazacos and her research team developed the all-vanadium RFB (V-RFB), which used the same vanadium element in both half-cells, to prevent cross-contamination. The all-vanadium RFB's patent was submitted by the UNSW research team in 1986. The first generation of the V-RFB system developed at UNSW focused on different material components of the batter, modeling and simulation methods, control strategies, and cell stack design, generating over 30 patents [67], [68], [69]. In 1993, UNSW issued Gypsum, Thailand the license to start the first field test of the V-RFB system. A 2 kW/12 kWh V-RFB system was integrated into a 1 kW rooftop PV system in Thailand to demonstrate the self-sufficiency of the PV-battery system in place of a PV-diesel system [70]. In 1998, Pinnacle VRB, a firm located in Australia bought the UNSW's V-RFB patents to further develop the V-RFB technology. Pinnacle issued a license to Sumitomo Electric Industries, Japan that successfully commissioned over 20 V-RFB systems ranging from medium-scale to large-scale applications including the 4 MW/6 MWh V-RFB installed at the Subaru Wind Farm, Japan in 2005. When the basic patent for the V-RFB expired in 2006, the research and development of the V-RFB experienced significant progress that has led to the commercialization of various V-RFB projects worldwide [71], [72], [73], over 700 MWh of V-RFBs have been installed worldwide by 2021 and more projects are underway [74]. Table 2 presents some of the recent V-RFB projects that have been commissioned or are ongoing.

III. BASIC WORKING PRINCIPLE AND COMPONENTS OF A V-RFB SYSTEM

A. OPERATION OF V-RFBs

The V-RFB is a type of flow battery that uses the different oxidation states in the vanadium ions to store chemical energy. A typical V-RFB system consists of electrodes (anode and cathode), electrolyte, ion membrane, circulation pumps, and storage tanks as shown in Fig. 1 [75], [76]. The electrodes which are separated by the membrane are housed in the cell stack while the circulation pump is used in each half cell (positive and negative) to drive the electrolyte from the storage tank into the cell stack where the electrochemical reaction occur. The electrolyte in the storage tank for the positive half-cell is a pair of VO2+/VO+2 (V4+/V5+) while the negative half-cell electrolyte is a pair of V2+/V3+, the vanadium-based electrolytes in both half-cells are dissolved in sulfuric acid as a supporting electrolyte.

During the discharge electrochemical process, the positive half-cell undergoes a reduction reaction, i.e., gain of an electron on the surface of the anode as given by

$$VO_2^+ + e^- + 2H^+ \leftrightarrow VO^{2+} + H_2O \quad E^0 = 1.004\ \text{V}. \quad (1)$$

In the negative half-cell, an oxidation reaction, i.e., loss of an electron, occurs on the surface of the cathode to convert V^{2+} ions to V^{3+} ion. This electrochemical process can be expressed as

$$V^{2+} \leftrightarrow V^{3+} + e^- \quad E^0 = -0.255\ \text{V}. \quad (2)$$

The overall electrochemical reaction can be written as

$$VO_2^+ + 2H^+ + V^{2+} \leftrightarrow VO^{2+} + H_2O + V^{3+} \quad E^0 = 1.259\ \text{V}, \quad (3)$$

where $\leftrightarrow$ represents a reversible reaction (charge and discharge). The reversible electrode reactions must be at the same rate where the rate of oxidation is equal to the rate of reduction under balanced conditions. The cell open circuit voltage can be deduced from the Nernst equation using [77] and [78]

$$E_{OCV} = E^0 + \frac{\text{RT}}{zF} \ln \left[\frac{C_{V^{5+}} (C_{H^+})^2 C_{V^{2+}}}{C_{V^{3+}} C_{V^{4+}}} \right], \quad (4)$$

where E^0 is the standard electrode potential, R is the universal gas constant, F is Faraday's constant, T is the thermodynamic temperature in Kelvin, z is the number of electrons transferred in the overall redox reaction, C_V is the concentration of the different vanadium ions, and C_{H^+} is the concentration of the protons. The state of charge (SoC) of the V-RFB is dependent on the concentration of the vanadium ions in the electrolytes, this can be defined as

$$SoC = \frac{C_{V^{2+}}}{C_{V^{2+}} + C_{V^{3+}}} = \frac{C_{V^{5+}}}{C_{V^{4+}} + C_{V^{5+}}}. \quad (5)$$

From (5), the Nernst equation in (4) can be rewritten as

$$E_{OCV} = E^0 + \frac{\text{RT}}{zF} \ln \left[\frac{SoC}{1 - SoC} \right]. \quad (6)$$

In a V-RFB stack, there are a number of individual cells connected together in series. The stack terminal voltage for a V-RFB system consisting of N_{cell} number of cells can be expressed as

$$E_{stack} = N_{cell} E_{OCV} - E_{loss}, \quad (7)$$

where E_{loss} is the total voltage loss in the stack that can be expressed as

$$E_{loss} = E_{ohm} + E_{act} + E_{tr} + E_{cr}, \quad (8)$$

where E_{ohm} is the ohmic loss as a result of the current passing through the components in the stack, E_{act} is the activation loss as a result of the reaction polarization at the electrode, E_{tr} is the transfer loss as a result of the concentration variation

TABLE 2. Recent V-RFB projects and their applications.

Reference	Name of Project	Size	Location	Year	RE Integration	Applications
[55]	Hubei Storage Integration Demonstration Project	10 MW/ 40 MWh	China	2017	PV and Wind	• Improve the quality of power supply from the RE sources • Reduce peak load on grid • Reduce emissions
[56]	Hesteel Project	5 kW/ 20 kWh	China	2020	PV	• Peak shaving • Improve clean energy utilization • reduce emissions • Reduce overall fossil energy consumption
[57]	Scottish Water Project	800 kWh	UK	2022	PV and Wind	• Improve the quality of power supply from the RE sources
[58]	Energy Superhub Project	2 MW/5 MWh	UK	2022	None	• Load shifting • Grid support
[59]	Yadlamlka Energy Project (Ongoing)	8 MWh	Australia	2022	PV	• PV power shifting • Local grid frequency support
[60]	Dalian City	100 MW/400 MWh	China	2022	None	• Reduce peak load on grid • Improve power quality • Increase size of RE on the grid
[61]	Elemental Energy	2.8 MW/8.4 MWh	Canada	2022	PV	• Improve PV efficiency • Grid support • Increase flexibility of the system
[62]	Automobile Industrial Park (Ongoing)	100 MW/ 500 MWh	China	2023	PV	• Grid support
[63]	H2 Project (Ongoing)	20 MWh	USA	2023	Gas plant	• Grid support • Reduce power generation from gas plant • Reduce emissions from gas plant
[64]	G&W Electric (Ongoing)	2 MW/8 MWh	USA	2023	PV	• Provide more reliable power during seasonal peak demands • actively participate in power utility demand response program

between the electrolyte and the surface of the electrode, and E_{cr} is the crossover loss as a result of the ion passage in the membrane and the shunt current [79], [80], [81]. To reduce the stack voltage loss and improve the performance of the V-RFB system, an improvement in the material and components of the V-RFB is required [82].

B. MAJOR COMPONENTS AND MATERIALS OF V-RFBs

1) ELECTROLYTE

The electrolyte is a major active material in the V-RFB system, it stores energy in its chemical forms and its concentration level determines the energy capacity of the system. In a typical V-RFB, the electrolyte is a mixture of different oxidation states of vanadium and supporting additives such as hydrochloric (HCl) acid, sulphuric (H_2SO_4), etc [83]. The functions of the supporting electrolytes are to increase the conductivity of the main electrolyte and transfer hydrogen ions for the positive half-cell reaction as shown in (1). The conventional H_2SO_4-based V-RFBs have the limitation of low energy density as a result of the poor solubility and stability of the vanadium solution [84]. Research to improve the energy density and performance of the V-RFB by using different supporting electrolytes have been reported in [84], [85], [86], [87], [88], [89], [90], [91], [92], and [93]. In [85], four different organic additives, di-sorbitol, fructose, glucose, and mannitol, are investigated to prevent the precipitation of the VO_2^+/VO^{2+} electrolyte. It was observed that the di-sorbitol additive produced the best performance with a slightly higher EE of 82% in contrast to 80% EE for the electrolyte without additives. In [86], two organic additives –inositol and phytic acid– are used to improve the electrochemical reversibility of the VO_2^+/VO^{2+} electrolyte. It was reported that the organic additives improved the thermal stability of electrolytes. In [87], amino-methyl sulfonic acid (AMSA) and methane-sulfonic acid (MSA) are employed as organic additives for the electrolytes. However, [84] postulated that organic additives cannot provide the significant development that will increase the marketability of the V-RFB for large-scale renewable energy applications. Thus, inorganic additives have been used to improve the

electrochemical process of the electrolyte. In [88], potassium-diformate (KDF) is added to the electrolyte to increase the thermal stability of the electrolyte. The results of the experiments showed that the KDF-based electrolyte maintained approximately 99% of its concentration at $60°C$ compared to the traditional electrolyte solution at 88% concentration. Authors in [89] prepared the all-vanadium electrolyte using ammonium-metavanadate (AMV) as the additive electrolyte. Other inorganic additives such as sodium pyrophosphate tetrabasic (SPT) [90], boric acid [91], methacrylic acid [92], ammonium phosphate [93] have been adopted to improve the electrochemical potency and stability of the electrolyte at high temperatures.

2) ELECTRODE

Another important component of the V-RFB that affects its applications and market penetration is the electrode. Compared to conventional electrochemical batteries such as Li-ion and lead-acid batteries where the electrodes are active agents in the electrochemical reactions, the electrodes in the V-RFBs do not actively partake in the electrochemical reaction, rather they act as a surface for the reaction to occur. Therefore, to harness a high electrochemical reaction on the electrode surface area, the electrodes in the V-RFB must have certain characteristics such as large surface area and electrochemical window, high conductivity and electrochemical reaction activity, good chemical stability, and cheap [94], [95], [96]. The review in [97] revealed that the improvement in electrode surface with low cost will increase the large-scale engineering applications and commercialization of the V-RFB technology. Since the development of the first V-RFB in the 1980s, carbon-based materials, carbon-polymer composites, and non-carbon materials have been investigated and used for the electrodes in the positive and negative half cells of the V-RFB. Experiments have shown that carbon-based materials such as carbon felts, carbon paper, carbon nanotubes, graphite felts, and graphene are the most suitable due to their high electrical conductivity, high specific surface area, and low cost [98].

To reduce the concentration polarization that causes the activation voltage loss, and improve electrochemical reversibility and catalytic activity on the surface of the electrodes, several modification strategies have been proposed. The electrode modification strategies based on the increase in surface area [99], [100], [101], [102], the introduction of surface functional groups [103], [104], [105], [106], the introduction of electrocatalyst [107], [108], [109], [110], and optimization of the microstructure [111], [112], [113], [114] have been investigated. To reduce the ohmic voltage loss that is caused by the ohmic polarization (internal resistance) in the V-RFBs, porous electrode structures have been introduced [115], [116], [117]. Since the ohmic voltage loss increases as the operating current increases, it is expected that the ohmic losses will be higher in large-scale V-RFB applications. Thus, it is necessary to reduce the thickness of the electrodes to reduce the ohmic loss; some works have developed techniques to address this issue. However, it should be noted that reducing the thickness of the electrode will reduce its surface area, leading to an increase in concentration and electrochemical polarization. Therefore, optimal electrode thickness must be selected to achieve the best performance and efficiency.

3) MEMBRANE

The ion membrane is another important component of the V-RFB and has a significant impact on the performance of the battery. It separates the positive half-cell from the negative half-cell to prevent the cross-transportation of electrolytes. It is also responsible for completing the electrical circuit by transporting protons [118]. An ideal membrane should have a low permeability to mitigate the rate of self-discharge, high ion conductivity to dampen the ohmic loss during the transport of protons, and low production cost - the membrane accounts for 44% and 27% of the total cost of 250 kWh and 4 MWh V-RFBs, respectively [119], [120]. The movement of protons in the membrane is based on the principle of convection, diffusion, and migration [121], [122]. To reduce cross-contamination –a major cause of performance deterioration in V-RFBs, it is important to investigate the transport mechanism of ions to optimize the performance of the V-RFB. Studies in [123], [124], [125], [126], and [127] have presented various transport models that can increase the efficiency of the V-RFB system.

Nafion is the most widely used material for the membrane of V-RFBs because of its high conductivity and good chemical stability. However, it is highly permeable and expensive, making it unsuitable for large-scale applications [128], [129]. Different kinds of membranes including cation exchange membrane [130], [131], [132], [133], anion exchange membrane [134], [135], [136], [137], amphoteric ion exchange membrane [138], [139], [140], [141], and porous membranes [142], [143], [144], [145] have been proposed and developed for V-RFB systems.

C. PERFORMANCE EVALUATION METRICS OF V-RFBs

In practical applications of batteries, it is impossible for the battery to have the same charge and discharge capacity. Thus, it is important to evaluate the performance of the battery based on its efficiency. The charging and discharging operations are the widely used methods for evaluating the performance of a battery. The battery can be charged or discharged in constant current (CC) mode, constant voltage (CV) mode, or constant power (CP) mode.

In CC mode, the charge or discharge current is constant while the voltage and power rise(charge) or decline(discharge). In the CV mode, the charge or discharge voltage is constant while the current and power decline in both operations because the difference between the OCV and charge/discharge voltage gets smaller as the process continues. In CP mode, power is fixed during the charge and discharge operations. In the charge operation, the current

declines while the voltage rises. In the discharge operation, the current rises as the voltage declines. Based on the simplicity of the CC mode to study the performance of V-RFB systems, it has been widely used to evaluate the performance and efficiency of V-RFB systems. In this section, we consider four efficiency metrics that are applicable to all ESS technologies and an additional metric that is specific to RFB systems [146], [147]:

1) COULOMB EFFICIENCY

The coulomb efficiency (CE) is defined as the ratio of the discharged ampere-hours (Ah) to the charged Ah. It can be mathematically expressed as

$$CE = \frac{Ah_{disch}}{Ah_{ch}} \times 100\% = \frac{\int_0^{t_d} I_{disch} dt}{\int_0^{t_c} I_{ch} dt} \times 100\%. \quad (9)$$

where I_{disch} is the discharge current, I_{ch} is the charge current, t_c and t_d are the charge and discharge times, respectively. Compared to solid-state ESS such as Li-ion batteries where the CE indicates the capacity loss per cycle which is a vital metric to predict the remaining battery life, the CE evaluation in V-RFBs measures the ratio of the charge and discharge capacities for a given cycle. Thus, it is difficult to predict the life cycle of the V-RFB using the CE because of the reversibility of the vanadium species. The higher the CE, the less capacity in *Ah* that the V-RFB loses in a specific charge/discharge cycle. Experiments in [148] showed that at a constant flow rate, the CE of the V-RFB stack increases as the current density increases. In practice, the CE is determined by charging and discharging the battery at specified voltage limits and taking note of the time taken for the charge and discharge operation. The drawback of this method is that it does factor in the capacity loss during the cycling between charge and discharge operations. Instead of using the voltage limits to compute the CE, another approach is to use the SoC limits of the V-RFB to determine its CE since any decline in the battery's capacity is usually reflected in the SoC [149].

2) VOLTAGE EFFICIENCY

Voltage efficiency (VE) is defined as the ratio of the average discharge voltage to the average charging voltage. It can be mathematically expressed as

$$VE = \frac{V_{disch}^{avg}}{V_{ch}^{avg}} \times 100\%. \quad (10)$$

The VE evaluates the effect of cell voltage losses during the charge/discharge cycle. The losses resulting from the ohmic resistance, reaction polarization of electrodes, and concentration overpotential as given in (7) reduce the VE of the battery. The SoC of the battery also plays a significant role in determining the VE of the battery as given in (6). Since the ohmic losses increase as the stack current increases, the VE decreases with an increase in the current density of the V-RFB stack. The VE of the V-RFB can be increased by reducing the cell resistance (reduce ohmic loss), utilizing materials with good electroactivity (reduce reaction polarization) and high electrical conductivity (reduce concentration overpotential) for the electrodes [150]. Studies suggest that optimizing the flow rate in the V-RFB stack can increase the VE because the concentration overpotential is reduced, thus the battery can operate at a lower voltage during the charge period and a higher voltage during the discharge period [148].

3) ENERGY EFFICIENCY

Energy efficiency (EE) is defined as the ratio of discharge energy in watt-hour (Wh) to the charged energy. It can be mathematically expressed as

$$EE = \frac{Wh_{disch}}{Wh_{ch}} \times 100\% = \frac{\int_0^{t_d} I_{disch} \cdot V_{disch} dt}{\int_0^{t_c} I_{ch} \cdot V_{ch} dt} \times 100\%. \quad (11)$$

The EE of the battery represents its energy conversion capability. A high EE indicates a strong energy conversion capability. As the cycling (charge/discharge) operation of the V-RFB increases, the EE of the battery degrades. This is mostly a result of the deterioration in the surface properties of the electrodes during the redox reaction. One direct way to recover the EE of the V-RFB is to replace the deteriorated electrodes. However, the drawback of this method is the increase in the maintenance cost of the V-RFB system. Another cost-effective method to recover the EE of a V-RFB system is to interchange the electrodes, i.e., the positive electrode now becomes the negative electrode and vice-versa [151]. The relationship between the CE, EE, and VE is given as

$$EE = CE \times VE. \quad (12)$$

4) SYSTEM EFFICIENCY

The system efficiency (SE) of a V-RFB system is defined as the ratio of the net output power during discharge to the net power consumed while charging. It can be mathematically expressed as

$$SE = \frac{P_{disch}^{net}}{P_{ch}^{net}} \times 100\% \quad (13)$$

In contrast to EE, the SE accounts for the parameters such as pump power consumption, cooling system power consumption, and power consumption from other auxiliaries in the V-RFB system that participate in the charge and discharge operations. Following this, the SE can be calculated from

$$SE = \frac{P_{disch} - P_{disch}^{aux}}{P_{ch} + P_{ch}^{aux}} \times 100\%, \quad (14)$$

where P_{dish} the average discharge power by the battery, P_{ch} is the average charge power of the batter, P_{disch}^{aux} and P_{ch}^{aux} are the auxiliary power consumption during the discharge and charge operations, respectively.

5) ELECTROLYTE UTILIZATION

Electrode utilization is defined as the ratio of the actual capacity of the electrolyte to the calculated capacity of the

electrolyte. It can be mathematically expressed as

$$\text{Electrolyte Utilization} = \frac{Wh_{actual}}{Wh_{calc}} \times 100\% \quad (15)$$

The electrolyte utilization is a reflection of the V-RFB capacity since the capacity of the V-RFB is a function of the concentration and volume of the electrolyte. The electrolyte utilization represents the utilization of the active species in the electrolyte. Due to the power and capacity decoupling in V-RFB systems, the increase in volume or concentration increases the capacity of the battery without altering the stack configuration (electrode surface area and stack number) of the V-RFB system. As the number of charge/discharge cycles increases, the capacity of the V-RFB reduces. Conventionally, the capacity of the battery can be restored by remixing the anolyte and catholyte, then starting the splitting all over again. During the electrolyte splitting, it is important that the anolyte and catholyte are divided into two equal parts [151].

IV. MODELING METHODS OF V-RFB SYSTEMS

In this section, the modeling techniques of V-RFBs are discussed. Generally, the study of V-RFBs can be divided into four stages depending on the objective of the study and area of interest [152], [153]. The first stage is the material stage, which involves the material modeling and analysis of the components such as electrodes, electrolytes, and membranes. The second stage is the cell stage, which involves modeling methods based on the interaction of the different components in the V-RFB cell. The interactions may include heat transfer, mass transport, and other physicochemical reactions in the cell. The third stage is the system stage, which will be buttressed in this section, it involves modeling methods based on the electrochemical process of the V-RFB. It relates to flow rate, cell stack design, and electrical and thermal processes in the V-RFB stack. The last stage is the market stage, which involves modeling methods based on the commercialization of the V-RFB stack. It relates to the capacity loss, cost analysis, life cycle, and safety measures of the V-RFB system [154]. The system-level modeling is the most appropriate to study the practicality of V-RFBs for renewable energy and power systems applications [43], [155]. In the early stages of V-RFB developments, small-scale laboratory experiments and field testing are used to investigate their performance. The major drawback of these approaches is to difficulty to quantify their economies of scale under different operating conditions and applications. The use of simulation tools to model the V-RFB system will aid a more thorough investigation of system performance under varied testing conditions.

A. EQUIVALENT CIRCUIT MODEL

The equivalent electric circuit model has shown accurate results to represent the behavior of the V-RFB for system-level analysis. The method uses the basic electrical components to model the system. The advantage of this approach is that it reduces the computational complexity for solving the physicochemical process of the V-RFB but the accurate methods for parameter estimation and identification still pose a challenge. Most works rely on experimental or field data for cross-validation. The generic equivalent circuit model of a V-RFB stack consists of internal resistance that represents the losses based on the bipolar plate, electrode, mass transfer, membrane, and reaction kinetics; the parasitic resistance represents the circulation pump power loss and by-pass current power loss [156], [157], [158]. It can be divided in to three subsystems;(i) Stack voltage (E_{stack}) subsystem, (ii) SoC estimator subsystem, and (iii) flow rate subsystem.

The E_{stack} is based on the Nernst equation in (6) and (7). Since the SoC of the V-RFB depends on the concentration (energy capacity) of the electrolyte in the tank, (5) can be redefined as

$$SoC = \frac{\text{Instantaneous Energy}}{\text{Total Energy Capacity}}. \quad (16)$$

Under balance conditions of the electrolytes, the SoC can be expressed as

$$SoC(t) = SoC(t-1) + \Delta SoC, \quad (17)$$

where $SoC(t-1)$ is the initial SoC and ΔSoC is the change in SoC that is a function of the current flowing in the stack (I_{stack}) and the capacity of electrolyte remaining in the tank.

The circulation pump is used to pump the electrolyte from the tank into the stack, it is important to model the dynamics of the flow rate (Q) that can be mathematically expressed as

$$Q = \frac{I_{stack}}{SoC \times C_{elect}}, \quad (18)$$

where C_{elect} is the electrolyte capacity.

In [159], the proposed equivalent circuit model uses a voltage source to represent the stack voltage, and a controlled current source in parallel with a resistor to represent the pump losses. In [160], the extended Kalman filter was used for parameter identification of unknown parameters in the equivalent circuit. The simulation results were consistent with the field data. The model did not consider the impacts of parameters that are dynamic in the practical operation of the system. The real-time simulation of the equivalent model was presented in [161], but the impact of self-discharge was not covered. The self-discharge behavior was explored in [162] using the equivalent circuit model, although the model did investigate the effects of vanadium ions crossover over the membrane and the impact of the dynamic flow rate on the EE was not considered. A detailed equivalent circuit model of the V-RFB was proposed in [163] to obtain internal parameters by fitting the experimental data into the model. The self-discharge phenomenon and ion crossing were taken into consideration in the model. The effect of the flow rate on the internal resistance of the V-RFB stack was also discussed. To evaluate the effect of the pump and shunt current losses, the model proposed in [164] used a resistor connected in series and parallel to represent the shunt current circuit and used the hydraulic model equation to design the pump model.

To estimate the unknown parameters, the experimental results in [165] were used. In [166], the dynamic equivalent circuit of the V-RFB that considered the SoC, operational cycle number, and flow rate of the stack was proposed. The internal parameters of the systems were extracted using parameter identification from a 1 kW/6kWh V-RFB system. The major drawback of the previously proposed equivalent circuit models is the assumption of constant operating temperature, which is impractical.

B. THERMAL MODEL

Modeling the thermal behavior of the V-RFB is important in understanding the practical dynamics of the battery in order to develop an efficient battery management system. The temperature rise in the V-RFB stack is primarily a result of the heat generated by the internal resistance of the stack during charging and discharging operations. The thermal model of the V-RFB is based on the principle of mass transfer theory and thermodynamics equations can be expressed as [167] and [168]

$$C_{\mathrm{P}}\rho V_{\mathrm{s}}\frac{\mathrm{d}T_{\mathrm{s}}}{\mathrm{d}t} = Q^{+}C_{\mathrm{P}}\rho\left(T^{+}-T^{\mathrm{s}}\right)+Q^{-}C_{\mathrm{P}}\rho\left(T^{-}-T^{\mathrm{s}}\right) + I_{\mathrm{ch}}^{2}R_{\mathrm{ch}}, \tag{19}$$

$$C_{\mathrm{P}}\rho V_{\mathrm{s}}\frac{\mathrm{d}T_{\mathrm{s}}}{\mathrm{d}t} = Q^{+}C_{\mathrm{P}}\rho\left(T^{+}-T^{\mathrm{s}}\right)+Q^{-}C_{\mathrm{P}}\rho\left(T^{-}-T^{\mathrm{s}}\right) + I_{\mathrm{disch}}^{2}R_{\mathrm{disch}}, \tag{20}$$

$$C_{\mathrm{P}}\rho V^{+}\frac{\mathrm{d}T_{\mathrm{S}}}{\mathrm{d}t} = Q^{+}C_{\mathrm{P}}\rho\left(T^{\mathrm{s}}-T^{+}\right)+U^{+}A^{+}\left(T^{\mathrm{a}}-T^{+}\right), \tag{21}$$

$$C_{\mathrm{P}}\rho V^{-}\frac{\mathrm{d}T^{\mathrm{s}}}{\mathrm{d}t} = Q^{-}C_{\mathrm{P}}\rho\left(T^{\mathrm{s}}-T^{-}\right)+U^{-}A^{-}\left(T^{\mathrm{a}}-T^{-}\right), \tag{22}$$

where C_p is the specific heat of the electrolytes, ρ is the density of the electrolyte, V_s, V^+, and V^- are the volumes of the battery stack, catholyte tank, and anolyte tank, respectively; T^s, T^+, T^-, and T^a are the temperatures of the battery stack, catholyte tank, anolyte tank, and ambient temperatures, respectively; Q^+ and Q^- are the flow rates of the catholyte and anolyte; U^+ and U^- are the heat transfer coefficients of the catholyte and anolyte; A^+ and A^- are the surface areas of the catholyte and anolyte tanks; I_{ch} and I_{disch} are the charging and discharging currents; R_{ch} and R_{disch} are the total internal resistances of the stack during charging and discharging cycles. Equivalent thermal models that characterize the impacts of parasitic pump losses and shunt current have been investigated. A 3-D nonisothermal model of the V-RFB was developed in [169] to study the heat generated in form of entropic heat, joule heat, and overpotential at different current densities. The results showed that the cathode generated more heat than the anode during the charge and discharge operations. In [170] and [171], the 2-D model was developed and the results were similar to the 3-D model. Three metaheuristic algorithms – ant lion algorithm, genetic algorithm, and particle swarm algorithm– were used for parameter identification of the thermal model developed in [172].

In order to investigate the coupling effect of different models of the V-RFB under varying operating conditions, a hybrid model of V-RFBs has been developed.

C. HYBRID MODEL

The existing modeling of V-RFB is being improved to hybrid models that provide realistic simulation characteristics for the analysis of large-scale V-RFBs required for renewable energy applications. The hybrid models may consider a combination of the chemical characteristics, electrical characteristics, thermal characteristics, and other features of the V-RFB to develop a comprehensive model that can accurately predict the performance of the V-RFB under a wide range of operating scenarios. Authors in [173] proposed a thermal-hydraulic hybrid model of the V-RFB. The model was used to estimate the temperature of the electrolytes under different current densities and ambient temperatures. In [174], an electrothermal model including a cooling strategy was developed. Their analysis showed that the temperature of the electrolyte was impacted by the flow rate of the coolant which improves the CE, EE, and VE of the battery. An optimized hybrid model was proposed in [175] for the operation of the V-RFB in a microgrid with high penetration of renewable energy. The model comprises electrochemical and fluid dynamics models to obtain the efficiency of the battery, an economic model was then formulated by considering the economic benefits, investment costs, operation costs, and renewable energy utilization in the microgrid. By considering the electrochemical equations, electrode kinetics equation, membrane kinetics equation, and flow dynamics kinetics equations, a multiphysics model of the V-RFB was developed to analyze the performance and efficiency of the battery for renewable energy applications. In the hybrid model developed in [176], the equivalent circuit is used to model the electrical behavior of the battery, the electrochemical model is used to reflect the chemical behavior of the battery, and the hydrodynamic model is used to reflect the effect of the flow of the battery. The accuracy of the proposed model was verified by comparison with experimental data.

A major challenge in the modeling of the V-RFB system is the estimation of the key parameter of the model that guarantees its accuracy. Also, some of the parameters of the V-RFB cannot be measured in real-time, causing modeling errors. Therefore, a complementary modeling approach is usually deployed for the V-RFB system. In this approach, the known parameters of the developed models are validated with the experimental data, and the unknown parameters are estimated using the developed models. This guarantees proper emulation of the V-RFBs with minimum error and aids the development of an accurate battery management system (BMS) for the V-RFB system. For example, accurate estimation of the SoC ensures the proper charging and discharging operation of the battery while accurate estimation of the stack temperature can mitigate the risk of electrolyte precipitation, reducing the

TABLE 3. Parameter identification methods for V-RFB models.

Reference	Model	Estimated Parameter(s)	Estimation/Identification Method
[160]	Equivalent Circuit Model	• Open circuit voltage • Polarization losses	Extended Kalman Filter
[164]	Hybrid Model	• SoC fading • Stack voltage • Pump power losses	Least Squares Method
[171]	Thermal Model	• Cell stack temperature distribution	Experimental Validation
[172]	Thermal Model	• Heat transfer coefficients • Electrolyte temperature • Stack temperature	Genetic Algorithm, Particle Swarm Optimization, and Ant Lion Optimization
[174]	Hybrid Model	• Electrolyte temperature • Terminal voltage	Genetic Algorithm
[180]	Equivalent Circuit Model	• SoC • Capacity fading factor	Sliding Mode Observer
[181]	Equivalent Circuit Model	• Ohmic resistance • Polarization loss • SoC	Unscented Kalman Filter and Recursive Least Squares Algorithm
[182]	Hybrid Model	• Electrolyte temperature • SoC • Terminal voltage	Extended Kalman Filter
[183]	Equivalent Circuit Model	• Peak power	Extended Kalman Filter and Recursive Least Squares
[184]	Hybrid Model	• Flow rate • Open circuit voltage	PI and Robust controllers
[185]	Thermal Model	• Stack temperature	Lookup table
[186]	Thermal Model	• Cell stack temperature • Shunt current	Curve fitting
[187]	Equivalent Circuit Model	• Stack power loss • Pump power loss	Linear Regression, Support vector regression, and Ensemble learning-Adaptive boost algorithms
[188]	Electrochemical model	• Electrolyte flow rate	Gain scheduling
[189]	Hybrid Model	• Flow rate • Pump losses • Stack temperature	Empirical Data
[190]	Hybrid Model - Real-time data extraction	• SoC • Battery capacity	Back propagation neural network

risk of a fire incident. It is important to mention that the BMS of the V-RFB system has similar functions –cell monitoring, SoC estimation, protection, charging and discharging operation, local diagnosis, and data management– with conventional ESS technologies with the addition of the flow rate management [177], [178], [179]. Table 3 provides the parameter identification techniques that have been used in V-RFB models to improve the BMS of the battery technology.

V. SYSTEM-LEVEL PERFORMANCE IMPROVEMENT OF V-RFB SYSTEMS FOR RENEWABLE ENERGY APPLICATIONS

The majority of the research and developments have focused on the material level such as electrode design, electrolyte improvement, ion membrane design, and current collectors. However, the key technical parameters that affect the large-scale integration of the V-RFBs are at the system level and market level [191].

A. EFFECT OF SHUNT CURRENT IN V-RFBs

In the operation of the V-RFBs, the circulation pumps transport the electrolytes into the stack through the manifolds and flow channels. Owing to the conducting characteristics of the electrolytes, shunt currents are generated within the flow channels, manifolds, and inside the piping system. There are two major problems associated with shunt currents inside the V-RFB stack. First, they corrode the materials in the V-RFB stack, shortening the V-RFB's cycle life. Additionally, they reduce the V-RFB stack's ability to transfer energy, which results in the reduction of the CE of the battery [192]. They can also increase the stack's temperature beyond safe operating limits. Experiments on a 9 kW/27 kWh V-RFB system showed that the shunt current losses are about 20 times higher than the pump losses [193]. Therefore, methods to measure and reduce shunt currents are required to increase the large-scale applications of the V-RFB system. Shunt currents are usually impacted by the number of individual cells in the stack, the number of stacks in the system, SoC, operating current, the equivalent resistance of the electrolyte in the flow channel and manifold, and the piping structure of the system. The CE of a V-RFB was reduced from 99% to 80% when the number of cells in the stack was increased from 5 to 40 [194]. Analysis of the work conducted in [195] concluded that decreasing the number of individual cells in the stack and increasing the power of each cell in the stack can reduce the shunt current losses. In the instance of a bipolar stack design, the presence of shunt currents has a direct impact on the battery performance. Higher efficiency is guaranteed by a proper stack design with reduced shunt current. Authors in [196] studied how the shunt current affected the performance of a 40-cell 5 kW V-RFB stack when it was in idle mode. While they did not examine the impact of the shunt current at the cell level, they did study the temperature effect of the shunt current, which caused the temperature within the V-RFB stack to increase. Since the industrial-level V-RFB stack consists of a sizable number of cells, it was necessary to determine how the shunt current affected the individual cells. In [186], a numerical thermal model that calculated the shunt current losses caused by the internal channels and manifolds linking identical cell electrodes was developed. Due to the difference in cell potentials in the stack, electrical loops are formed on the path provided by the internal channels and manifolds for the flow of electrolytes. These electrical loops receive the shunt current that raises the temperature profile of the stack. By extending the channel of the V-RFB stack and decreasing the cross-sectional area of the manifold of the V-RFB cell, the shunt current loss can be reduced. It is worth noting that the pressure loss is directly proportional to the channel's length [197]. Strategies to reduce the shunt current losses include decreasing the electrolyte's conductivity, reworking the geometry of the flow channel and cell manifold, optimizing the piping system, and optimal stack design [194], [198].

B. EFFECT OF FLOW RATE IN V-RFBs

The flow rate, Q, is the rate at which circulation pumps deliver electrolytes into the V-RFB stack. The flow rate is a major feature of the V-RFB to increase its application at the macro level. The flow rate is affected by the SOC, electrolyte capacity, and stack current as given in (18). Studies have shown that improving the flow rate and flow field structure of the V-RFB reduces the concentration polarization, an increase the EE, and the overall performance of the battery [199]. A lower flow rate increases the battery polarization which reduces the terminal voltage of the battery stack as expressed in (8). Furthermore, the pressure difference between the outlet and inlet valves of the electrolyte channel is directly proportional to the flow rate of the electrolyte. It was experimentally shown in [185] that is important to maintain the flow rate at a higher level to ensure complete charge and discharge operations. A strategy to increase the flow rate at the end of charge and discharge operations while maintaining a constant flow rate was proposed in [200]. While this method increases the EE of the battery, it reduces its system efficiency because of the increase in pump losses. Since the concentration overpotential and the pump losses are impacted by the flow rate, using the flow channel design to minimize shunt current can potentially have a detrimental effect by increasing energy losses. Therefore, a trade-off between flow rate optimization and stack design is required to minimize parasitic losses and achieve higher system efficiency. In [201], a variable flow rate strategy was developed to ensure an optimal trade-off between the concentration overpotential and the pump losses while maintaining the stack temperature with safe limits. A flow rate optimization framework under different charge and discharge conditions was developed in [202]. The framework was developed based on the multi-physics model of the V-RFB and validated using real-time data. To guarantee robustness to dynamic parametric changes that occur in practical V-RFBs, several closed-loop flow rate strategies including PI control [188], robust feedback control [184], online dynamic optimization [203], fuzzy logic control [204] have been proposed for optimal flow rate in the V-RFB stack to reduce the pump losses and obtain good dynamic characteristics of the system under varying conditions.

C. EFFECT OF STACK DESIGN

The stack of the V-RFB is an important part that needs to be strategically designed to improve the performance of the system. The stack design is affected by the number of cells, the size of individual cells, and the flow channel configuration. For a given stack, the current density and EE vary under varying output power. Thus, the current density, output power of the stack, and the EE must be considered during the stack design. While the stack output power can be increased by increasing the size of the electrodes, this increases the cost of the stack. Similarly, an increase in cell size will increase the output power of the stack, this will also impact the uniformity

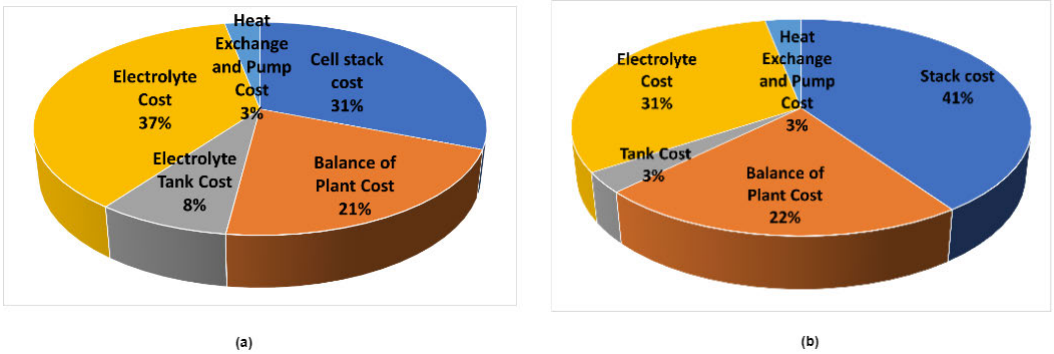

FIGURE 2. Variation in Capital Cost of V-RFB (a) [205] (b) [206].

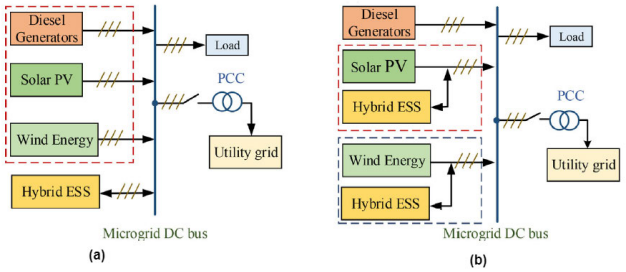

FIGURE 3. V-RFB ESS configuration (a) centralized (b) distributed [211].

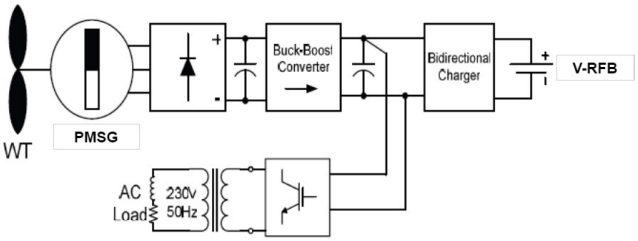

FIGURE 4. Stand-alone PMSG-based wind turbine with V-RFB integration [156].

in the flow rate of the electrolyte over a long flow path which increases the pump losses [207]. A low-loss stack topology was proposed in [208] using different cell and stack arrangements to evaluate the shunt current losses in a V-RFB system. A parallel-series cell configuration was adopted to increase the terminal voltage and reduce the shunt current losses. The multi-stack design investigated in [209] showed that the shunt current between stacks increases the shunt current within stacks leading to a decrease in CE of the V-RFB system. In a multi-stack system, the overall efficiency of the system is determined by the stack with the least efficiency. Therefore, the cell arrangement in the stack to achieve optimal efficiency of the system is crucial. In [210], the effect of cell layout on the performance of a multi-stack system was studied. Thirty-five possible cell layouts for an eight-stack system were considered during the experiments. The result showed that the CE of the system can be improved by grouping cells with similar internal resistances into stacks. The reduction of the internal resistance of the stack via cell layout reconfiguration, increasing the electrolyte conductivity, and optimal flow rate are ways to increase the stack performance of the V-RFB system.

D. COST IMPLICATION OF V-RFBs

Despite the wide range of benefits of the V-RFB ESS, its large-scale implementation has been significantly hampered by cost. It is not completely understood which components of the V-RFB have the most contribution to the overall. Some studies suggest that a significant portion of the capital cost of a V-RFB is from the cost of the electrolyte as shown in Figure 2(a) [205] while others suggest that the cell stack accounts for the highest proportion of cost in the V-RFB system as shown in Figure 2(b) [206]. Studies performed in [212] showed that the replacement cost of the membrane inside a V-RFB stack is around 15% of the initial investment costs. Therefore, the cost-benefit or techno-economic analysis of the V-RFB is crucial to investigate its economic benefits for large-scale applications. For the techno-economic analysis of ESS investments, the Levelized cost of storage (LCOS) is a metric that is used to evaluate the discounted cost per unit of discharged energy. It takes into account the economic and technical parameters that directly affect the cost of discharging stored energy in ESS over its lifetime, similar to the Levelized cost of electricity (LCOE) in traditional generation technologies [213]. The LCOS represents the average cost at which the stored energy in the ESS can be sold to get at least a zero net present value. The LCOS in $/MWh can be evaluated using [214]

$$LCOS = \frac{IC + \sum_{n=1}^{N} \frac{OC+CC+EC}{(1+r)^n}}{\sum_{n=1}^{N} \frac{E_{disch}}{(1+r)^n}} \tag{23}$$

where IC is the investment cost; OC is the operation cost; EC is the end-of-life cost; r is the discount rate; N is the lifetime of the ESS. The IC is computed from the energy capacity and nominal power of the ESS, cost of energy, and cost of replacement. The OC takes into account the cost of operation and maintenance which is relative to the capacity of the battery. The CC is calculated from the round-trip

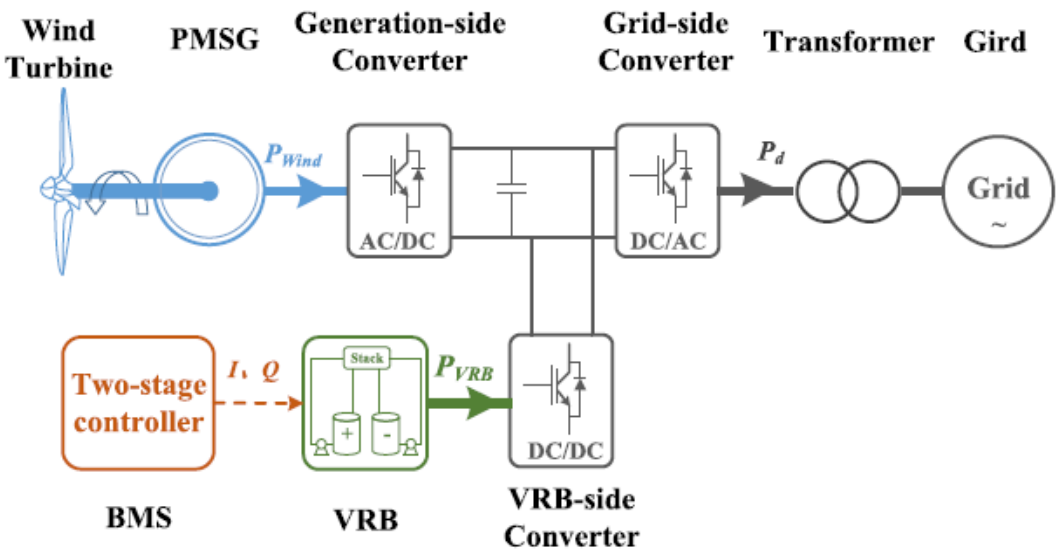

FIGURE 5. Diagram of grid-connected PMSG-based wind/V-RFB system [191].

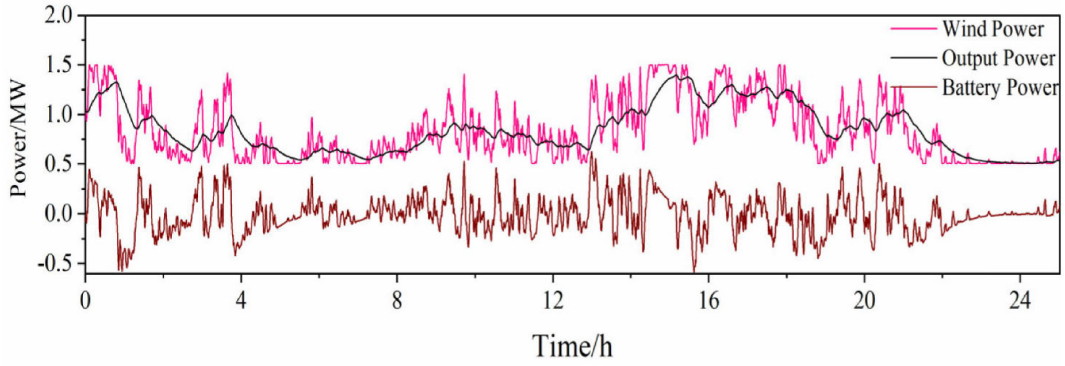

FIGURE 6. Output of wind power and V-RFB power during power smoothing [191].

efficiency and price of electricity while the EC is computed as a fraction of the investment cost [214]. A cost-benefit analysis using the LCOS was conducted in [214] for nine ESS technologies including the V-RFB for twelve different ESS applications such as energy arbitrage, primary response, secondary response, tertiary response, black start, power reliability, bill management, peaker replacement, seasonal storage, power quality, congestion management, and transmission and & distribution investment deferral. The techno-economic study conducted in [215] showed that using RFBs with inexpensive materials is cost-advantageous for long discharge applications exceeding eight hours compared to other ESS technologies. It also revealed that the high efficiency and high power density of the V-RFB makes it technically impressive in minimizing its LCOS compared to other RFB technologies. However, the study did not include the capacity loss of the V-RFB in the LCOS formulation. The cost-benefit framework that incorporates the capacity fading and re-balancing characteristics of the V-RFB was developed in [216]. The results of the analysis identified avenues such as a re-balancing schedule, reducing fade rates, optimal battery sizing, and electrolyte leasing as methods of cost reduction in the V-RFB.

In contrast to other ESS technology, the long life cycle of the V-RFB allows for a trade-off between the initial investment cost and lifetime operating cost to achieve optimal LCOS. For medium and large-scale commercial applications, the economic analyses showed that the V-RFB has a high net profit margin despite its high capital cost [217].

VI. APPLICATION OF V-RFBs WITH RENEWABLE ENERGY SYSTEMS

As aforementioned that the V-RFB has been used in RE-based systems for different applications such as power smoothing, peak shaving, improving power quality, grid support, etc. In this section, we discuss some of the applications of

V-RFBs in PV and wind-based RE systems. In grid-connected microgrids, V-RFBs, as with other ESS, can be connected in three different configurations as shown in Figure 3 [211]. In the centralized configuration shown in Figure 3(a), the total power of the ESS is delivered to the grid via the point of common coupling (PCC). If the V-RFB is to achieve power smoothing of the aggregated RE output power at the PCC, the capacity of the storage required would increase, thereby increasing the cost of the V-RFB setup for large-scale RE systems. In the distributed configuration shown in Figure 3(b), the energy storage is connected to individual RE sources before connecting to the PCC. The distributed configuration makes the control of the V-RFB easier, and it prevents the problem of excessively scaling the storage capacity as in the centralized configuration.

In [156], a 5 kW/20 kWh V-RFB system is connected to a stand-alone 3 kW wind energy system with a permanent magnet synchronous generator (PMSG) on the DC side as shown in Figure 4. In the setup, the AC output from the wind turbine is rectified to DC and connected to the output of the bi-directional charger controller of the V-RFB, the AC load is supplied from the inverter that is connected to the common DC output of the power supplies (wind turbine and battery). When the load is greater than the power from the wind turbine, the battery discharges to offset the power deviation on the system. Similarly, when the wind turbine generates more power than the power, the excess power is used to charge the battery for another cycle of operation. For grid-connected applications, a 600 kW/1200 kWh V-RFB is integrated with a 2 MW grid-connected PMSG-based wind turbine system as shown in Figure 5 [191]. The V-RFB was deployed for power smoothing of the wind turbine output as shown in Figure 6. To achieve power smoothing, the high-frequency component of the output power from the wind turbine is absorbed by the V-RFB, and the smoothened wind power is supplied to the grid. Similarly, a V-RFB was employed for power smoothing of a grid-connected doubly fed induction generator (DFIG)-based wind farm in [218]. Results show that the V-RFB responds to filter the gust power from the wind farm before the action of the pitch angle controller that has a larger time constant. The fast response characteristics of the V-RFB system for a grid-connected PV system were investigated in [219]. The analysis was carried out under different SoC, flow rate, and load conditions. In the discharge mode of the V-RFB, two timescales (20 ms and 120 ms) were investigated for a fast response such as primary frequency regulation. The results showed that the V-RFB can provide fast services to the 50/60 Hz grid if the discharge current is driven in the constant current-source mode by the bi-directional converter interface of the V-RFB system. For protection services, the V-RFB is connected to the DC link of the full power converter of a wound rotor synchronous generator (WRSG)-based wind turbine to enhance its low-voltage ride-through capability [220].

VII. CONCLUSION AND FUTURE DIRECTIONS

The emerging changes in modern power systems structure and operations require the adoption of energy storage systems, especially to enable higher penetration of renewable energy systems without compromising the stability and resilience of the entire system. This review has covered the current state of V-RFB technology in research and industry. The recent and ongoing projects are presented. It covers the working principle, design, and constraints of the major component and research to increase the operating efficiency of each component in the V-RFB system. The importance of accurate and hybrid modeling schemes has been emphasized. These hybrid modeling schemes will provide scope for evaluating various parameters of the V-RFB under different operating conditions in order to improve the overall system efficiency. While significant progress has been made over time in the research and development of V-RFB systems, the current technologies still do not meet the requirements for large-scale power systems applications. Advancements are required at all levels (materials, cell, system, and market) of the V-RFB modeling to improve its capability for commercial applications.

- Research in practical vanadium-based electrolytes with higher energy density, stability, and a wider range of operating temperatures is required for the increased commercialization of the V-RFBs for large-scale applications.
- Advanced research to increase the electrochemical reactions at the electrode surface is required. The effect of the ohmic loss, activation loss, and concentration should be thoroughly investigated. New techniques to determine the optimal surface area of the electrodes to increase the power density would be beneficial.
- Continuous effort to improve the flow rate strategy in a large-scale multi-stack V-RFB is required to reduce the pump losses and improve the overall performance of the system.
- Advanced methods to determine the optimal cell and stack arrangements of large-scale V-RFB systems to increase the output power without compromising its EE are required.
- Advanced multi-physics modeling methods are required to understand the dynamic behavior of the V-RFBs under varying conditions. Real-time Accurate and realistic modeling are needed to understand and investigate the practical operation of large-scale V-RFBs in different grid scenarios.
- A major limitation to the market penetration of the V-RFB is cost. Therefore, all methods to improve the overall efficiency and performance of the system must be cost-effective.

REFERENCES

[1] "World energy outlook 2021," IEA, Paris, 2021. [Online]. Available: https://www.iea.org/reports/world-energy-outlook-2021

[2] A. O. Aluko, R. Musumpuka, and D. G. Dorrell, "Cyberattack-resilient secondary frequency control scheme for stand-alone microgrids," *IEEE Trans. Ind. Electron.*, vol. 70, no. 2, pp. 1622–1634, Feb. 2023.
[3] A. Aluko, R. P. Carpanen, D. Dorrell, and E. Ojo, "Virtual inertia control strategy for high renewable energy-integrated interconnected power systems," in *Proc. Int. Conf. Electr. Electron. Eng.*, Cham, Switzerland: Springer, 2022, pp. 346–364.
[4] A. G. Olabi, C. Onumaegbu, T. Wilberforce, M. Ramadan, M. A. Abdelkareem, and A. H. Al-Alami, "Critical review of energy storage systems," *Energy*, vol. 214, Jan. 2021, Art. no. 118987.
[5] A. G. Olabi and M. A. Abdelkareem, "Energy storage systems towards 2050," *Energy*, vol. 219, Mar. 2021, Art. no. 119634.
[6] F. Nadeem, S. M. Hussain, P. K. Tiwari, A. K. Goswami, and T. S. Ustun, "Comparative review of energy storage systems, their roles, and impacts on future power systems," *IEEE Access*, vol. 7, pp. 4555–4585, 2019.
[7] O. Krishan and S. Suhag, "An updated review of energy storage systems: Classification and applications in distributed generation power systems incorporating renewable energy resources," *Int. J. Energy Res.*, vol. 43, no. 12, pp. 6171–6210, Oct. 2019.
[8] M. T. L. Parimi and A. V. P. Kumar, "A review of reactive power compensation techniques in microgrids," *Renew. Sustain. Energy Rev.*, vol. 81, pp. 1030–1036, Jan. 2018.
[9] D.-I. Stroe, V. Knap, M. Swierczynski, A.-I. Stroe, and R. Teodorescu, "Operation of a grid-connected lithium-ion battery energy storage system for primary frequency regulation: A battery lifetime perspective," *IEEE Trans. Ind. Appl.*, vol. 53, no. 1, pp. 430–438, Jan./Feb. 2017.
[10] M. Farhadi and O. Mohammed, "Energy storage technologies for high-power applications," *IEEE Trans. Ind. Appl.*, vol. 52, no. 3, pp. 1953–1961, May/Jun. 2016.
[11] M. A. Hannan, S. B. Wali, P. J. Ker, M. S. A. Rahman, M. Mansor, V. K. Ramachandaramurthy, K. M. Muttaqi, T. M. I. Mahlia, and Z. Y. Dong, "Battery energy-storage system: A review of technologies, optimization objectives, constraints, approaches, and outstanding issues," *J. Energy Storage*, vol. 42, Oct. 2021, Art. no. 103023.
[12] H. Chen, T. N. Cong, W. Yang, C. Tan, Y. Li, and Y. Ding, "Progress in electrical energy storage system: A critical review," *Prog. Natural Sci.*, vol. 19, no. 3, pp. 291–312, 2009.
[13] A. A. Kebede, T. Kalogiannis, J. Van Mierlo, and M. Berecibar, "A comprehensive review of stationary energy storage devices for large scale renewable energy sources grid integration," *Renew. Sustain. Energy Rev.*, vol. 159, May 2022, Art. no. 112213.
[14] J. Mitali, S. Dhinakaran, and A. A. Mohamad, "Energy storage systems: A review," *Energy Storage Saving*, vol. 1, no. 3, pp. 166–216, Sep. 2022.
[15] W. He, M. King, X. Luo, M. Dooner, D. Li, and J. Wang, "Technologies and economics of electric energy storages in power systems: Review and perspective," *Adv. Appl. Energy*, vol. 4, Nov. 2021, Art. no. 100060.
[16] M. Arbabzadeh, J. X. Johnson, G. A. Keoleian, P. G. Rasmussen, and L. T. Thompson, "Twelve principles for green energy storage in grid applications," *Environ. Sci. Technol.*, vol. 50, no. 2, pp. 1046–1055, Jan. 2016.
[17] Z. Zhang, T. Ding, Q. Zhou, Y. Sun, M. Qu, Z. Zeng, Y. Ju, L. Li, K. Wang, and F. Chi, "A review of technologies and applications on versatile energy storage systems," *Renew. Sustain. Energy Rev.*, vol. 148, Sep. 2021, Art. no. 111263.
[18] E. Bazdar, M. Sameti, F. Nasiri, and F. Haghighat, "Compressed air energy storage in integrated energy systems: A review," *Renew. Sustain. Energy Rev.*, vol. 167, Oct. 2022, Art. no. 112701.
[19] C. R. Matos, P. P. Silva, and J. F. Carneiro, "Overview of compressed air energy storage projects and regulatory framework for energy storage," *J. Energy Storage*, vol. 55, Nov. 2022, Art. no. 105862.
[20] K. M. Tan, T. S. Babu, V. K. Ramachandaramurthy, P. Kasinathan, S. G. Solanki, and S. K. Raveendran, "Empowering smart grid: A comprehensive review of energy storage technology and application with renewable energy integration," *J. Energy Storage*, vol. 39, Jul. 2021, Art. no. 102591.
[21] A. G. Olabi, Q. Abbas, A. Al Makky, and M. A. Abdelkareem, "Supercapacitors as next generation energy storage devices: Properties and applications," *Energy*, vol. 248, Jun. 2022, Art. no. 123617.
[22] A. G. Olabi, T. Wilberforce, E. T. Sayed, A. G. Abo-Khalil, H. M. Maghrabie, K. Elsaid, and M. A. Abdelkareem, "Battery energy storage systems and SWOT (strengths, weakness, opportunities, and threats) analysis of batteries in power transmission," *Energy*, vol. 254, Sep. 2022, Art. no. 123987.
[23] G. J. May, A. Davidson, and B. Monahov, "Lead batteries for utility energy storage: A review," *J. Energy Storage*, vol. 15, pp. 145–157, Feb. 2018.
[24] I. Iwakiri, T. Antunes, H. Almeida, J. P. Sousa, R. B. Figueira, and A. Mendes, "Redox flow batteries: Materials, design and prospects," *Energies*, vol. 14, no. 18, p. 5643, Sep. 2021.
[25] D. Zhang, Q. Liu, and Y. Li, "Design of flow battery," in *Reactor and Process Design in Sustainable Energy Technology*. Amsterdam, The Netherlands: Elsevier, 2014, pp. 61–97.
[26] R. Ye, D. Henkensmeier, S. J. Yoon, Z. Huang, D. K. Kim, Z. Chang, S. Kim, and R. Chen, "Redox flow batteries for energy storage: A technology review," *J. Electrochemical Energy Convers. Storage*, vol. 15, no. 1, Feb. 2018.
[27] O. Nolte, I. A. Volodin, C. Stolze, M. D. Hager, and U. S. Schubert, "Trust is good, control is better: A review on monitoring and characterization techniques for flow battery electrolytes," *Mater. Horizons*, vol. 8, no. 7, pp. 1866–1925, 2021.
[28] A. M. Fenton, R. K. Jha, B. J. Neyhouse, A. P. Kaur, D. A. Dailey, S. A. Odom, and F. R. Brushett, "On the challenges of materials and electrochemical characterization of concentrated electrolytes for redox flow batteries," *J. Mater. Chem. A*, vol. 10, no. 35, pp. 17988–17999, 2022.
[29] J. Houser, A. Pezeshki, J. T. Clement, D. Aaron, and M. M. Mench, "Architecture for improved mass transport and system performance in redox flow batteries," *J. Power Sources*, vol. 351, pp. 96–105, May 2017.
[30] C. Ponce de León, A. Frías-Ferrer, J. González-García, D. A. Szánto, and F. C. Walsh, "Redox flow cells for energy conversion," *J. Power Sources*, vol. 160, no. 1, pp. 716–732, Sep. 2006.
[31] M. Skyllas-Kazacos, M. H. Chakrabarti, S. A. Hajimolana, F. S. Mjalli, and M. Saleem, "Progress in flow battery research and development," *J. Electrochemical Soc.*, vol. 158, no. 8, p. R55, 2011.
[32] A. Z. Weber, M. M. Mench, J. P. Meyers, P. N. Ross, J. T. Gostick, and Q. Liu, "Redox flow batteries: A review," *J. Appl. Electrochemistry*, vol. 41, no. 10, pp. 1137–1164, Sep. 2011.
[33] L. Li, S. Kim, W. Wang, M. Vijayakumar, Z. Nie, B. Chen, J. Zhang, G. Xia, J. Hu, G. Graff, J. Liu, and Z. Yang, "A stable vanadium redox-flow battery with high energy density for large-scale energy storage," *Adv. Energy Mater.*, vol. 1, no. 3, pp. 394–400, May 2011.
[34] G. L. Soloveichik, "Flow batteries: Current status and trends," *Chem. Rev.*, vol. 115, no. 20, pp. 11533–11558, Oct. 2015.
[35] M. Park, J. Ryu, W. Wang, and J. Cho, "Material design and engineering of next-generation flow-battery technologies," *Nature Rev. Mater.*, vol. 2, no. 1, pp. 1–18, Nov. 2016.
[36] O. C. Esan, X. Shi, Z. Pan, X. Huo, L. An, and T. S. Zhao, "Modeling and simulation of flow batteries," *Adv. Energy Mater.*, vol. 10, Jun. 2020, Art. no. 2000758.
[37] M. Rychcik and M. Skyllas-Kazacos, "Characteristics of a new all-vanadium redox flow battery," *J. Power Sources*, vol. 22, no. 1, pp. 59–67, Jan. 1988.
[38] R. K. Sankaralingam, S. Seshadri, J. Sunarso, A. I. Bhatt, and A. Kapoor, "Overview of the factors affecting the performance of vanadium redox flow batteries," *J. Energy Storage*, vol. 41, Sep. 2021, Art. no. 102857.
[39] H. Zhang, X. Li, and J. Zhang, *Redox Flow Batteries: Fundamentals and Applications*. Boca Raton, FL, USA: CRC Press, 2017.
[40] L. Cao, A. Kronander, A. Tang, D.-W. Wang, and M. Skyllas-Kazacos, "Membrane permeability rates of vanadium ions and their effects on temperature variation in vanadium redox batteries," *Energies*, vol. 9, no. 12, p. 1058, Dec. 2016.
[41] R. Schweiss, A. Pritzl, and C. Meiser, "Parasitic hydrogen evolution at different carbon fiber electrodes in vanadium redox flow batteries," *J. Electrochemical Soc.*, vol. 163, no. 9, pp. A2089–A2094, 2016.
[42] L. Wei, T. S. Zhao, Q. Xu, X. L. Zhou, and Z. H. Zhang, "*in-situ* investigation of hydrogen evolution behavior in vanadium redox flow batteries," *Appl. Energy*, vol. 190, pp. 1112–1118, Mar. 2017.
[43] A. A. Shah, H. Al-Fetlawi, and F. C. Walsh, "Dynamic modelling of hydrogen evolution effects in the all-vanadium redox flow battery," *Electrochimica Acta*, vol. 55, no. 3, pp. 1125–1139, Jan. 2010.
[44] L. Thaller, "Electrically rechargeable redox flow cell," NASA Lewis Research Center, Cleveland, OH, USA, Tech. Rep. 19770007638, 1976.
[45] L. Swette and V. Jalan, "Development of electrodes for the NASA iron/chromium redox system and factors affecting their performance," Giner, Inc., Waltham, MA, USA, Tech. Rep. DOE/NASA-0262-1; NASA-CR-174724, 1984.

[46] W. Wang, S. Kim, B. Chen, Z. Nie, J. Zhang, G.-G. Xia, L. Li, and Z. Yang, "A new redox flow battery using Fe/V redox couples in chloride supporting electrolyte," *Energy Environ. Sci.*, vol. 4, no. 10, pp. 4068–4073, 2011.

[47] W. Wang, Z. Nie, B. Chen, F. Chen, Q. Luo, X. Wei, G.-G. Xia, M. Skyllas-Kazacos, L. Li, and Z. Yang, "A new Fe/V redox flow battery using a sulfuric/chloric mixed-acid supporting electrolyte," *Adv. Energy Mater.*, vol. 2, no. 4, pp. 487–493, Apr. 2012.

[48] J. Noack, N. Roznyatovskaya, T. Herr, and P. Fischer, "The chemistry of redox-flow batteries," *Angew. Chem. Int. Ed.*, vol. 54, no. 34, pp. 9776–9809, 2015.

[49] M. Ravikumar, S. Rathod, N. Jaiswal, S. Patil, and A. Shukla, "The renaissance in redox flow batteries," *J. Solid State Electrochem.*, vol. 21, no. 9, pp. 2467–2488, 2017.

[50] P. Leung, X. Li, C. P. De León, L. Berlouis, C. J. Low, and F. C. Walsh, "Progress in redox flow batteries, remaining challenges and their applications in energy storage," *Rsc Adv.*, vol. 2, no. 27, pp. 10125–10156, 2012.

[51] R. J. Remick and P. G. Ang, "Electrically rechargeable anionically active reduction-oxidation electrical storage-supply system," U.S. Patent 4 485 154, Nov. 27, 1984.

[52] M. Skyllas-Kazacos, "Flow batteries: Vanadium and beyond," in *Redox Flow Batteries*. Boca Raton, FL, USA: CRC Press, 2017, pp. 327–354.

[53] F. C. Walsh, C. P. de Léon, L. Berlouis, G. Nikiforidis, L. F. Arenas-Martínez, D. Hodgson, and D. Hall, "The development of Zn-Ce hybrid redox flow batteries for energy storage and their continuing challenges," *ChemPlusChem*, vol. 80, no. 2, pp. 288–311, Feb. 2015.

[54] *Vizn Energy System*. Accessed: Nov. 1, 2022. [Online]. Available: http://www.viznenergy.com/technology/

[55] *Pu Neng Wins Contract for the Largest Vanadium Flow Battery in China*. Newsfile. Accessed: Nov. 1, 2022. [Online]. Available: https://www.newsfilecorp.com/release/30156/

[56] *VRB Energy Commissions 5 kW Vanadium Redox Battery Energy Storage System*. VRB Energy. Accessed: Nov. 2, 2022. [Online]. Available: https://vrbenergy.com/

[57] *Energy Superhub Oxford Invinity Energy Systems*. Accessed: Nov. 1, 2022. [Online]. Available: https://invinity.com/scottish-water-case-study/

[58] *Energy Superhub Oxford Invinity Energy Systems*. Accessed: Nov. 1, 2022. [Online]. Available: https://invinity.com/energy-superhub-oxford/

[59] *Yadlamalka Energ Project Invinity Energy Systems*. Accessed: Nov. 1, 2022. [Online]. Available: https://invinity.com/yadlamalka-energy/

[60] C. Andy. *First Phase of 800MWh World Biggest Flow Battery Commissioned in China Energy Storage News*. Accessed: Nov. 1, 2022. [Online]. Available: https://www.energy-storage.news/

[61] *Canada's Largest Solar-Powered Vanadium Flow Battery Invinity Energy Systems*. Accessed: Nov. 1, 2022. [Online]. Available: https://invinity.com/

[62] B. Emiliano. *Work Begins on 100 MW/500 MWh Vanadium Flow Battery in China Pv Magazine*. Accessed: Nov. 1, 2022. [Online]. Available: https://www.pv-magazine.com/2021/09/01/work-begins-on-100-mw-500-mwh-vanadium-flow-battery-in-china/

[63] H2, Inc. *Launches 20-MWh Vanadium Redox Flow Battery Storage Project in California Energy Storage*. Accessed: Nov. 1, 2022. [Online]. Available: https://www.energytech.com/energy-storage/article/21212949/h2-inc-launches-20mwh-flow-battery-project-in-california

[64] *Cellcube VRFB Chosen for U.S. MICROGRID PROJECT Energy Storage Journal*. Accessed: Nov. 1, 2022. [Online]. Available: https://www.energystoragejournal.com/cellcube-vrfb-chosen-for-us-microgrid-project/

[65] R. F. Savinell and J. S. Wainwright, "Iron-based flow batteries," U.S. Patent PCT/US2012/040 429, Nov. 27, 2012.

[66] H. Zhang and C. Sun, "Cost-effective iron-based aqueous redox flow batteries for large-scale energy storage application: A review," *J. Power Sources*, vol. 493, May 2021, Art. no. 229445.

[67] A. Parasuraman, T. M. Lim, C. Menictas, and M. Skyllas-Kazacos, "Review of material research and development for vanadium redox flow battery applications," *Electrochimica Acta*, vol. 101, pp. 27–40, Jul. 2013.

[68] M. Skyllas-Kazacos and R. Robins, "All-vanadium redox battery," U.S. Patent 4 786 567, Nov. 22, 1986.

[69] M. Skyllas-Kazacos, "High energy density vanadium electrolyte solutions," U.S. Patent 7 078 123 B2, Oct. 22, 2006.

[70] C. Menictas, M. Skyllas-Kazacos, and T. M. Lim, *Advances in Batteries for Medium and Large-Scale Energy Storage: Types and Applications*. Amsterdam, The Netherlands: Elsevier, 2014.

[71] M. Ulaganathan, V. Aravindan, Q. Yan, S. Madhavi, M. Skyllas-Kazacos, and T. M. Lim, "Recent advancements in all-vanadium redox flow batteries," *Adv. Mater. Interface*, vol. 3, no. 1, Jan. 2016, Art. no. 1500309.

[72] Y. Shi, C. Eze, B. Xiong, W. He, H. Zhang, T. M. Lim, A. Ukil, and J. Zhao, "Recent development of membrane for vanadium redox flow battery applications: A review," *Appl. Energy*, vol. 238, pp. 202–224, Mar. 2019.

[73] L. Gubler, "Membranes and separators for redox flow batteries," *Current Opinion Electrochem.*, vol. 18, pp. 31–36, Dec. 2019.

[74] B. N. E. Finance. (2021). *Storage Data Hub Storage Asset*. [Online]. Available: https://about.bnef.com/

[75] A. Joseph, J. Sobczak, G. Żyła, and S. Mathew, "Ionic liquid and ionanofluid-based redox flow Batteries—A mini review," *Energies*, vol. 15, no. 13, p. 4545, Jun. 2022.

[76] E. Sánchez-Díez, E. Ventosa, M. Guarnieri, A. Trovò, C. Flox, R. Marcilla, F. Soavi, P. Mazur, E. Aranzabe, and R. Ferret, "Redox flow batteries: Status and perspective towards sustainable stationary energy storage," *J. Power Sources*, vol. 481, Jan. 2021, Art. no. 228804.

[77] A. Clemente, M. Montiel, F. Barreras, A. Lozano, and R. Costa-Castello, "Vanadium redox flow battery state of charge estimation using a concentration model and a sliding mode observer," *IEEE Access*, vol. 9, pp. 72368–72376, 2021.

[78] L. Wang, H.-Y. Gao, C.-W. Tseng, Z.-H. Huang, M.-F. Lee, Y.-S. Lin, H.-S. Huang, C.-C. Tseng, A. V. Prokhorov, H. B. Mokhlis, K. H. Chua, and M. Tripathy, "Small-signal stability analysis of a vanadium redox flow battery-based energy-storage system," in *Proc. IEEE Int. Future Energy Electron. Conf. (IFEEC)*, Nov. 2021, pp. 1–6.

[79] S. Yao, J. Zhou, Y. Zhang, J. Hu, and T. Xie, "Modeling and characterization of the biochar electrodes for vanadium redox flow battery," *Electrochimica Acta*, vol. 400, Dec. 2021, Art. no. 139469.

[80] G. Mourouga, D. Chery, E. Baudrin, H. Randriamahazaka, T. J. Schmidt, and J. O. Schumacher, "Estimation of activity coefficients for aqueous organic redox flow batteries: Theoretical basis and equations," *iScience*, vol. 25, no. 9, Sep. 2022, Art. no. 104901.

[81] W. W. Yang, Y. L. He, and Y. S. Li, "Performance modeling of a vanadium redox flow battery during discharging," *Electrochimica Acta*, vol. 155, pp. 279–287, Feb. 2015.

[82] N. M. Delgado, R. Monteiro, J. Cruz, A. Bentien, and A. Mendes, "Shunt currents in vanadium redox flow batteries—A parametric and optimization study," *Electrochimica Acta*, vol. 403, Jan. 2022, Art. no. 139667.

[83] P.-J. Alphonse, M. Tas, and G. Elden, "Numerical investigation of supporting electrolyte using in a vanadium redox flow battery," *ECS Meeting Abstr.*, vol. 1, no. 48, p. 2032, Jul. 2022.

[84] F. Rahman and M. Skyllas-Kazacos, "Evaluation of additive formulations to inhibit precipitation of positive electrolyte in vanadium battery," *J. Power Sources*, vol. 340, pp. 139–149, Feb. 2017.

[85] S. Li, K. Huang, S. Liu, D. Fang, X. Wu, D. Lu, and T. Wu, "Effect of organic additives on positive electrolyte for vanadium redox battery," *Electrochimica Acta*, vol. 56, no. 16, pp. 5483–5487, Jun. 2011.

[86] X. Wu, S. Liu, N. Wang, S. Peng, and Z. He, "Influence of organic additives on electrochemical properties of the positive electrolyte for all-vanadium redox flow battery," *Electrochimica Acta*, vol. 78, pp. 475–482, Sep. 2012.

[87] Z. He, J. Liu, H. Han, Y. Chen, Z. Zhou, S. Zheng, W. Lu, S. Liu, and Z. He, "Effects of organic additives containing NH_2 and SO_3H on electrochemical properties of vanadium redox flow battery," *Electrochimica Acta*, vol. 106, pp. 556–562, Sep. 2013.

[88] X. Wei, G. Wang, F. Li, J. Zhang, J. Chen, and R. Wang, "High performance positive electrolyte with potassium diformate (KDF) additive for vanadium redox flow batteries," *Int. J. Electrochem. Sci.*, vol. 17, Jan. 2022, Art. no. 220126.

[89] B.-Y. Jung, C.-H. Ryu, and G.-J. Hwang, "Characteristics of the all-vanadium redox flow battery using ammonium metavanadate electrolyte," *Korean J. Chem. Eng.*, vol. 39, no. 9, pp. 2361–2367, Sep. 2022.

[90] S.-K. Park, J. Shim, J. H. Yang, C.-S. Jin, B. S. Lee, Y.-S. Lee, K.-H. Shin, and J.-D. Jeon, "Effect of inorganic additive sodium pyrophosphate tetrabasic on positive electrolytes for a vanadium redox flow battery," *Electrochimica Acta*, vol. 121, pp. 321–327, Mar. 2014.

[91] G. Wang, J. Chen, X. Wang, J. Tian, H. Kang, X. Zhu, Y. Zhang, X. Liu, and R. Wang, "Study on stabilities and electrochemical behavior of V(V) electrolyte with acid additives for vanadium redox flow battery," *J. Energy Chem.*, vol. 23, no. 1, pp. 73–81, Jan. 2014.

[92] G. Wang, J. Zhang, J. Zhang, J. Chen, S. Zhu, X. Liu, and R. Wang, "Effect of different additives with –NH2 or –NH4+ functional groups on V(V) electrolytes for a vanadium redox flow battery," *J. Electroanal. Chem.*, vol. 768, pp. 62–71, May 2016.

[93] A. Mousa and M. Skyllas-Kazacos, "Effect of additives on the low-temperature stability of vanadium redox flow battery negative half-cell electrolyte," *ChemElectroChem*, vol. 2, no. 11, pp. 1742–1751, Nov. 2015.

[94] B. Escobar, D. C. Martínez-Casillas, K. Y. Pérez-Salcedo, D. Rosas, L. Morales, S. J. Liao, L. L. Huang, and X. Shi, "Research progress on biomass-derived carbon electrode materials for electrochemical energy storage and conversion technologies," *Int. J. Hydrogen Energy*, vol. 46, no. 51, pp. 26053–26073, Jul. 2021.

[95] H. Zhang, X. Li, and J. Zhang J, Eds., *Redox Flow Batteries: Fundamentals and Applications*. CRC Press, Nov. 2017.

[96] S. Sharma, A. K. Panwar, and M. Tripathi, "Storage technologies for electric vehicles," *J. Traffic Transp. Eng. English Ed.*, vol. 7, no. 3, pp. 340–361, 2020.

[97] D. M. Hall, R. M. Bachman, and L. R. Radovic, "Carbon materials in redox flow batteries: Challenges and opportunities," *Carbon Rep.*, vol. 1, no. 3, pp. 94–112, 2022.

[98] T. Liu, X. Li, H. Zhang, and J. Chen, "Progress on the electrode materials towards vanadium flow batteries (VFBs) with improved power density," *J. Energy Chem.*, vol. 27, no. 5, pp. 1292–1303, Sep. 2018.

[99] M. Schilling, M. Braig, K. Köble, and R. Zeis, "Investigating the V(IV)/V(V) electrode reaction in a vanadium redox flow battery—A distribution of relaxation times analysis," *Electrochimica Acta*, vol. 430, Oct. 2022, Art. no. 141058.

[100] T. Liu, X. Li, C. Xu, and H. Zhang, "Activated carbon fiber paper based electrodes with high electrocatalytic activity for vanadium flow batteries with improved power density," *ACS Appl. Mater. Interface*, vol. 9, no. 5, pp. 4626–4633, Feb. 2017.

[101] Y.-C. Chang, J.-Y. Chen, D. M. Kabtamu, G.-Y. Lin, N.-Y. Hsu, Y.-S. Chou, H.-J. Wei, and C.-H. Wang, "High efficiency of CO_2-activated graphite felt as electrode for vanadium redox flow battery application," *J. Power Sources*, vol. 364, pp. 1–8, Oct. 2017.

[102] D. M. Kabtamu, J.-Y. Chen, Y.-C. Chang, and C.-H. Wang, "Water-activated graphite felt as a high-performance electrode for vanadium redox flow batteries," *J. Power Sources*, vol. 341, pp. 270–279, Feb. 2017.

[103] M. E. Lee, D. Jang, S. Lee, J. Yoo, J. Choi, H.-J. Jin, S. Lee, and S. Y. Cho, "Silk protein-derived carbon fabric as an electrode with high electrocatalytic activity for all-vanadium redox flow batteries," *Appl. Surf. Sci.*, vol. 567, Nov. 2021, Art. no. 150810.

[104] I. Yang, S. Lee, D. Jang, J.-E. Lee, S. Y. Cho, and S. Lee, "Enhancing energy efficiency and long-term durability of vanadium redox flow battery with catalytically graphitized carbon fiber felts as electrodes by boron doping," *Electrochimica Acta*, vol. 429, Oct. 2022, Art. no. 141033.

[105] Z. He, Y. Lv, T. Zhang, Y. Zhu, L. Dai, S. Yao, W. Zhu, and L. Wang, "Electrode materials for vanadium redox flow batteries: Intrinsic treatment and introducing catalyst," *Chem. Eng. J.*, vol. 427, Jan. 2022, Art. no. 131680.

[106] J. Kim, H. Lim, J.-Y. Jyoung, E.-S. Lee, J. S. Yi, and D. Lee, "Effects of doping methods and kinetic relevance of n and o atomic co-functionalization on carbon electrode for V(IV)/V(V) redox reactions in vanadium redox flow battery," *Electrochimica Acta*, vol. 245, pp. 724–733, Aug. 2017.

[107] M. Steimecke, S. Rümmler, N.-F. Schuhmacher, T. Lindenberg, M. Hartmann, and M. Bron, "A comparative study of functionalized high-purity carbon nanotubes towards the V(IV)/V(V) redox reaction using cyclic voltammetry and scanning electrochemical microscopy," *Electroanalysis*, vol. 29, no. 4, pp. 1056–1061, Apr. 2017.

[108] P. M. Nia, E. Abouzari-Lotf, P. M. Woi, Y. Alias, T. M. Ting, A. Ahmad, and N. W. C. Jusoh, "Electrodeposited reduced graphene oxide as a highly efficient and low-cost electrocatalyst for vanadium redox flow batteries," *Electrochimica Acta*, vol. 297, pp. 31–39, Feb. 2019.

[109] X. Lu, F. Li, M. Steimecke, M. Tariq, M. Hartmann, and M. Bron, "Titanium as a substrate for three-dimensional hybrid electrodes for vanadium redox flow battery applications," *ChemElectroChem*, vol. 7, no. 3, pp. 737–744, Feb. 2020.

[110] Q. Zhang, T. Liu, H. Zhang, and X. Li, "Highly active Ag nanoparticle electrocatalysts toward V2+/V3+ redox reaction," *ACS Appl. Energy Mater.*, vol. 4, no. 4, pp. 3913–3920, Apr. 2021.

[111] A. Hassan and T. Tzedakis, "Enhancement of the electrochemical activity of a commercial graphite felt for vanadium redox flow battery (VRFB), by chemical treatment with acidic solution of $K_2Cr_2O_7$," *J. Energy Storage*, vol. 26, Dec. 2019, Art. no. 100967.

[112] K. Zhang, C. Yan, and A. Tang, "Oxygen-induced electrode activation and modulation essence towards enhanced anode redox chemistry for vanadium flow batteries," *Energy Storage Mater.*, vol. 34, pp. 301–310, Jan. 2021.

[113] D. O. Opar, R. Nankya, J. Lee, and H. Jung, "Three-dimensional mesoporous graphene-modified carbon felt for high-performance vanadium redox flow batteries," *Electrochimica Acta*, vol. 330, Jan. 2020, Art. no. 135276.

[114] J. Melke, J. Martin, M. Bruns, and P. Hügenell, A. Schökel, S. M. Isaza, F. Fink, P. Elsässer, and A. Fischer, "Investigating the effect of microstructure and surface functionalization of mesoporous N-doped carbons on V^{4+}/V^{5+} kinetics," *ACS Appl. Energy Mater.*, vol. 3, no. 12, pp. 11627–11640, 2020.

[115] M. Yue, Z. Lv, Q. Zheng, X. Li, and H. Zhang, "Battery assembly optimization: Tailoring the electrode compression ratio based on the polarization analysis in vanadium flow batteries," *Appl. Energy*, vol. 235, pp. 495–508, Feb. 2019.

[116] S. Aberoumand, P. Woodfield, B. Shabani, and D. V. Dao, "Advances in electrode and electrolyte improvements in vanadium redox flow batteries with a focus on the nanofluidic electrolyte approach," *Phys. Rep.*, vol. 881, pp. 1–49, Oct. 2020.

[117] A. Pathak, A. K. Sharma, and A. K. Gupta, "Dimensional analysis of a flow-by porous electrode and demonstration to all-vanadium redox flow batteries thereon," *J. Energy Storage*, vol. 44, Dec. 2021, Art. no. 103258.

[118] K. Shirasaki and T. Yamamura, "Direct observation of vanadium ion permeation behavior through Nafion 117 using 48 V radiotracer for all-vanadium redox flow battery," *J. Membrane Sci.*, vol. 592, Dec. 2019, Art. no. 117367.

[119] L. Zeng, T. S. Zhao, L. Wei, H. R. Jiang, and M. C. Wu, "Anion exchange membranes for aqueous acid-based redox flow batteries: Current status and challenges," *Appl. Energy*, vols. 233–234, pp. 622–643, Jan. 2019.

[120] Y. H. Wan, J. Sun, Q. P. Jian, X. Z. Fan, and T. S. Zhao, "A detachable sandwiched polybenzimidazole-based membrane for high-performance aqueous redox flow batteries," *J. Power Sources*, vol. 526, Apr. 2022, Art. no. 231139.

[121] A. R. Crothers, R. M. Darling, D. I. Kushner, M. L. Perry, and A. Z. Weber, "Theory of multicomponent phenomena in cation-exchange membranes: Part III. Transport in vanadium redox-flow-battery separators," *J. Electrochemical Soc.*, vol. 167, no. 1, Jan. 2020, Art. no. 013549.

[122] L. Hao, Y. Wang, and Y. He, "Modeling of ion crossover in an all-vanadium redox flow battery with the interfacial effect at membrane/electrode interfaces," *J. Electrochem. Soc.*, vol. 166, no. 8, pp. A1310–A1322, 2019.

[123] D. K. Kim, S. J. Yoon, and S. Kim, "Transport phenomena associated with capacity loss of all-vanadium redox flow battery," *Int. J. Heat Mass Transf.*, vol. 148, Feb. 2020, Art. no. 119040.

[124] C. A. Machado, G. O. Brown, R. Yang, T. E. Hopkins, J. G. Pribyl, and T. H. Epps, "Redox flow battery membranes: Improving battery performance by leveraging structure–property relationships," *ACS Energy Lett.*, vol. 6, no. 1, pp. 158–176, Jan. 2021.

[125] K. Oh, M. Moazzam, G. Gwak, and H. Ju, "Water crossover phenomena in all-vanadium redox flow batteries," *Electrochimica Acta*, vol. 297, pp. 101–111, Feb. 2019.

[126] X. L. Zhou, T. S. Zhao, L. An, Y. K. Zeng, and L. Wei, "Modeling of ion transport through a porous separator in vanadium redox flow batteries," *J. Power Sources*, vol. 327, pp. 67–76, Sep. 2016.

[127] X. L. Zhou, T. S. Zhao, L. An, Y. K. Zeng, and L. Wei, "Critical transport issues for improving the performance of aqueous redox flow batteries," *J. Power Sources*, vol. 339, pp. 1–12, Jan. 2017.

[128] K. Mushtaq, T. Lagarteira, A. A. Zaidi, and A. Mendes, "In-situ crossover diagnostics to assess membrane efficacy for non-aqueous redox flow battery," *J. Energy Storage*, vol. 40, Aug. 2021, Art. no. 102713.

[129] Y. Zhao, D. Zhang, L. Zhao, S. Wang, J. Liu, and C. Yan, "Excellent ion selectivity of Nafion membrane modified by PBI via acid-base pair effect for vanadium flow battery," *Electrochimica Acta*, vol. 394, Oct. 2021, Art. no. 139144.

[130] S. Thangarasu and T. H. Oh, "Progress in poly(phenylene oxide) based cation exchange membranes for fuel cells and redox flow batteries applications," *Int. J. Hydrogen Energy*, vol. 46, no. 77, pp. 38381–38415, Nov. 2021.

[131] P. T. Thong, K. V. Ajeya, K. Dhanabalan, S.-H. Roh, W.-K. Son, S.-C. Park, and H.-Y. Jung, "A coupled-layer ion-conducting membrane using composite ionomer and porous substrate for application to vanadium redox flow battery," *J. Power Sources*, vol. 521, Feb. 2022, Art. no. 230912.

[132] T. Sadhasivam, K. Dhanabalan, P. T. Thong, J. Kim, S. Roh, and H. Jung, "Development of perfluorosulfonic acid polymer-based hybrid composite membrane with alkoxysilane functionalized polymer for vanadium redox flow battery," *Int. J. Energy Res.*, vol. 44, no. 3, pp. 1999–2010, Mar. 2020.

[133] S. Hwang, D. Lee, Y. Rho, K. S. Yoon, D. M. Yu, S. J. Yoon, S. Kim, Y. T. Hong, and S. So, "Planar orientation of hydrophilic channels by biaxial deformation of perfluorinated sulfonic acid membranes for vanadium redox flow batteries," *J. Power Sources*, vol. 489, Mar. 2021, Art. no. 229497.

[134] S.-H. Roh, M.-H. Lim, T. Sadhasivam, and H.-Y. Jung, "Investigation on physico-chemical and electrochemical performance of poly(phenylene oxide)-based anion exchange membrane for vanadium redox flow battery systems," *Electrochimica Acta*, vol. 325, Dec. 2019, Art. no. 134944.

[135] E. J. Park, S. Maurya, U. Martinez, Y. S. Kim, and R. Mukundan, "Quaternized poly (arylene ether benzonitrile) membranes for vanadium redox flow batteries," *J. Membrane Sci.*, vol. 617, Jan. 2021, Art. no. 118565.

[136] A. Khataee, D. Pan, J. S. Olsson, P. Jannasch, and R. W. Lindström, "Asymmetric cycling of vanadium redox flow batteries with a poly(arylene piperidinium)-based anion exchange membrane," *J. Power Sources*, vol. 483, Jan. 2021, Art. no. 229202.

[137] M. Jung, W. Lee, C. Noh, A. Konovalova, G. S. Yi, S. Kim, Y. Kwon, and D. Henkensmeier, "Blending polybenzimidazole with an anion exchange polymer increases the efficiency of vanadium redox flow batteries," *J. Membrane Sci.*, vol. 580, pp. 110–116, Jun. 2019.

[138] S. Kumar, M. Bhushan, and V. K. Shahi, "Cross-linked amphoteric membrane: Sulphonated poly(ether ether ketone) grafted with 2,4,6-tris(dimethylaminomethyl)phenol using functionalized side chain spacers for vanadium redox flow battery," *J. Power Sources*, vol. 448, Feb. 2020, Art. no. 227358.

[139] Y. Chen, S. Zhang, Q. Liu, and X. Jian, "The effect of counter-ion substitution on poly (phthalazinone ether ketone) amphoteric ion exchange membranes for vanadium redox flow battery," *J. Membrane Sci.*, vol. 620, Feb. 2021, Art. no. 118816.

[140] Z. Bengui, Z. Yang, M. Zhao, Q. Liu, X. Zhang, Y. Fu, E. Zhang, K. Wang, G. Wang, Z. Zhang, and S. Zhang, "High-performance pyridine-containing fluorinated poly(aryl ether) membranes for vanadium flow batteries," *J. Power Sources*, vol. 542, Sep. 2022, Art. no. 231809.

[141] H. Zhang, Z. Li, L. Hu, L. Gao, M. Di, Y. Du, X. Yan, Y. Dai, X. Ruan, and G. He, "Covalent/ionic co-crosslinking constructing ultra-densely functionalized ether-free poly(biphenylene piperidinium) amphoteric membranes for vanadium redox flow batteries," *Electrochimica Acta*, vol. 359, Nov. 2020, Art. no. 136879.

[142] J. Balaji, M. G. Sethuraman, S.-H. Roh, and H.-Y. Jung, "Recent developments in sol-gel based polymer electrolyte membranes for vanadium redox flow batteries—A review," *Polym. Test.*, vol. 89, Sep. 2020, Art. no. 106567.

[143] X. Zhou, R. Xue, Y. Zhong, Y. Zhang, and F. Jiang, "Asymmetric porous membranes with ultra-high ion selectivity for vanadium redox flow batteries," *J. Membrane Sci.*, vol. 595, Feb. 2020, Art. no. 117614.

[144] L. Gubler, D. Vonlanthen, A. Schneider, and F. J. Oldenburg, "Composite membranes containing a porous separator and a polybenzimidazole thin film for vanadium redox flow batteries," *J. Electrochemical Soc.*, vol. 167, no. 10, Jan. 2020, Art. no. 100502.

[145] Q. Dai, W. Lu, Y. Zhao, H. Zhang, X. Zhu, and X. Li, "Advanced scalable zeolite 'ions-sieving' composite membranes with high selectivity," *J. Membrane Sci.*, vol. 595, Feb. 2020, Art. no. 117569.

[146] T. Puleston, A. Clemente, R. Costa-Castelló, and M. Serra, "Modelling and estimation of vanadium redox flow batteries: A review," *Batteries*, vol. 8, no. 9, p. 121, Sep. 2022.

[147] Z. Huang, A. Mu, L. Wu, and H. Wang, "Vanadium redox flow batteries: Flow field design and flow rate optimization," *J. Energy Storage*, vol. 45, Jan. 2022, Art. no. 103526.

[148] E. García-Quismondo, I. Almonacid, M. Á. C. Martínez, V. Miroslavov, E. Serrano, J. Palma, and J. P. A. Salmerón, "Operational experience of 5 kW/5 kWh all-vanadium flow batteries in photovoltaic grid applications," *Batteries*, vol. 5, no. 3, p. 52, Jul. 2019.

[149] A. Benjamin, E. Agar, C. R. Dennison, and E. C. Kumbur, "On the quantification of Coulombic efficiency for vanadium redox flow batteries: Cutoff voltages vs. state-of-charge limits," *Electrochemistry Commun.*, vol. 35, pp. 42–44, Oct. 2013.

[150] M. Skyllas-Kazacos, C. Menictas, and T. Lim, "Redox flow batteries for medium-to large-scale energy storage," in *Electricity Transmission, Distribution and Storage Systems*. Amsterdam, The Netherlands: Elsevier, 2013, pp. 398–441.

[151] L. Wei, X. Z. Fan, H. R. Jiang, K. Liu, M. C. Wu, and T. S. Zhao, "Enhanced cycle life of vanadium redox flow battery via a capacity and energy efficiency recovery method," *J. Power Sources*, vol. 478, Dec. 2020, Art. no. 228725.

[152] Q. Zheng, X. Li, Y. Cheng, G. Ning, F. Xing, and H. Zhang, "Development and perspective in vanadium flow battery modeling," *Appl. Energy*, vol. 132, pp. 254–266, Nov. 2014.

[153] X. Qiu, T. A. Nguyen, J. D. Guggenberger, M. L. Crow, and A. C. Elmore, "A field validated model of a vanadium redox flow battery for microgrids," *IEEE Trans. Smart Grids*, vol. 5, no. 4, pp. 1592–1601, Jul. 2014.

[154] N. Ra and A. Bhattacharjee, "An extensive study and analysis of system modeling and interfacing of vanadium redox flow battery," *Energy Technol.*, vol. 9, no. 1, Jan. 2021, Art. no. 2000708.

[155] K. Lourenssen, J. Williams, F. Ahmadpour, R. Clemmer, and S. Tasnim, "Vanadium redox flow batteries: A comprehensive review," *J. Energy Storage*, vol. 25, Oct. 2019, Art. no. 100844.

[156] L. Barote, C. Marinescu, and M. Georgescu, "VRB modeling for storage in stand-alone wind energy systems," in *Proc. IEEE Bucharest PowerTech*, Jun. 2009, pp. 1–6.

[157] Y. R. Challapuram, G. M. Quintero, S. B. Bayne, A. S. Subburaj, and M. A. Harral, "Electrical equivalent model of vanadium redox flow battery," in *Proc. IEEE Green Technol. Conference(GreenTech)*, Apr. 2019, pp. 1–4.

[158] F.-C. Gu, H.-C. Chen, and K.-Y. Li, "Mathematic modeling and performance analysis of vanadium redox flow battery," *Energy Fuels*, vol. 34, no. 8, pp. 10142–10147, Aug. 2020.

[159] J. Chahwan, C. Abbey, and G. Joos, "VRB modelling for the study of output terminal voltages, internal losses and performance," in *Proc. IEEE Canada Electr. Power Conf.*, Oct. 2007, pp. 387–392.

[160] M. R. Mohamed, H. Ahmad, M. N. A. Seman, S. Razali, and M. S. Najib, "Electrical circuit model of a vanadium redox flow battery using extended Kalman filter," *J. Power Sources*, vol. 239, pp. 284–293, Oct. 2013.

[161] B. Turker, S. A. Klein, L. Komsiyska, J. J. Trujillo, L. von Bremen, M. Kühn, and M. Busse, "Utilizing a vanadium redox flow battery to avoid wind power deviation penalties in an electricity market," *Energy Convers. Manage.*, vol. 76, pp. 1150–1157, Dec. 2013.

[162] B. W. Zhang, Y. Lei, B. F. Bai, and T. S. Zhao, "A two-dimensional model for the design of flow fields in vanadium redox flow batteries," *Int. J. Heat Mass Transf.*, vol. 135, pp. 460–469, Jun. 2019.

[163] M. Jarnut, S. Wermiński, and B. Waśkowicz, "Comparative analysis of selected energy storage technologies for prosumer-owned microgrids," *Renew. Sustain. Energy Rev.*, vol. 74, pp. 925–937, Jul. 2017.

[164] Y. Zhang, J. Zhao, P. Wang, M. Skyllas-Kazacos, B. Xiong, and R. Badrinarayanan, "A comprehensive equivalent circuit model of all-vanadium redox flow battery for power system analysis," *J. Power Sources*, vol. 290, pp. 14–24, Sep. 2015.

[165] S. Kim, E. Thomsen, G. Xia, Z. Nie, J. Bao, K. Recknagle, W. Wang, V. Viswanathan, Q. Luo, X. Wei, A. Crawford, G. Coffey, G. Maupin, and V. Sprenkle, "1 kW/1 kWh advanced vanadium redox flow battery utilizing mixed acid electrolytes," *J. Power Sources*, vol. 237, pp. 300–309, Sep. 2013.

[166] A. Bhattacharjee, A. Roy, N. Banerjee, S. Patra, and H. Saha, "Precision dynamic equivalent circuit model of a vanadium redox flow battery and determination of circuit parameters for its optimal performance in renewable energy applications," *J. Power Sources*, vol. 396, pp. 506–518, Aug. 2018.

[167] A. Tang, S. Ting, J. Bao, and M. Skyllas-Kazacos, "Thermal modelling and simulation of the all-vanadium redox flow battery," *J. Power Sources*, vol. 203, pp. 165–176, Apr. 2012.

[168] S. Han and L. Tan, "Thermal and efficiency improvements of all vanadium redox flow battery with novel main-side-tank system and slow pump shutdown," *J. Energy Storage*, vol. 28, Apr. 2020, Art. no. 101274.
[169] K. Oh, H. Yoo, J. Ko, S. Won, and H. Ju, "Three-dimensional, transient, nonisothermal model of all-vanadium redox flow batteries," *Energy*, vol. 81, pp. 3–14, Mar. 2015.
[170] B. W. Zhang, Y. Lei, B. F. Bai, A. Xu, and T. S. Zhao, "A two-dimensional mathematical model for vanadium redox flow battery stacks incorporating nonuniform electrolyte distribution in the flow frame," *Appl. Thermal Eng.*, vol. 151, pp. 495–505, Mar. 2019.
[171] A. Trovo, A. Saccardo, M. Giomo, and M. Guarnieri, "Thermal modeling of industrial-scale vanadium redox flow batteries in high-current operations," *J. Power Sources*, vol. 424, pp. 204–214, Jun. 2019.
[172] B. Khaki and P. Das, "Parameter identification of thermal model of vanadium redox batteries by Metaheuristic algorithms," *Electrochimica Acta*, vol. 394, Oct. 2021, Art. no. 139131.
[173] Z. Wei, J. Zhao, M. Skyllas-Kazacos, and B. Xiong, "Dynamic thermal-hydraulic modeling and stack flow pattern analysis for all-vanadium redox flow battery," *J. Power Sources*, vol. 260, pp. 89–99, Aug. 2014.
[174] Z. Wei, J. Zhao, and B. Xiong, "Dynamic electro-thermal modeling of all-vanadium redox flow battery with forced cooling strategies," *Appl. Energy*, vol. 135, pp. 1–10, Dec. 2014.
[175] J.-W. Ni, M.-J. Li, T. Ma, W. Wei, and Z. Li, "The configuration optimized design method based on real-time efficiency for the application of vanadium redox flow battery in microgrid," *Energy Convers. Manage.*, vol. 267, Sep. 2022, Art. no. 115899.
[176] S. Junkang, L. Xin, M. Yanqing, Q. Ya, D. Xueping, and Z. Haoyu, "Analysis of modeling and flow characteristics of vanadium redox flow battery," *Energy Storage Sci. Technol.*, vol. 9, no. 2, p. 645, 2020.
[177] H. Rahimi-Eichi, U. Ojha, F. Baronti, and M.-Y. Chow, "Battery management system: An overview of its application in the smart grid and electric vehicles," *IEEE Ind. Electron. Mag.*, vol. 7, no. 2, pp. 4–16, Jun. 2013.
[178] Y. Wang, J. Tian, Z. Sun, L. Wang, R. Xu, M. Li, and Z. Chen, "A comprehensive review of battery modeling and state estimation approaches for advanced battery management systems," *Renew. Sustain. Energy Rev.*, vol. 131, Oct. 2020, Art. no. 110015.
[179] H. Gabbar, A. Othman, and M. Abdussami, "Review of battery management systems (BMS) development and industrial standards," *Technologies*, vol. 9, no. 2, p. 28, Apr. 2021.
[180] B. Xiong, J. Zhao, Y. Su, Z. Wei, and M. Skyllas-Kazacos, "State of charge estimation of vanadium redox flow battery based on sliding mode observer and dynamic model including capacity fading factor," *IEEE Trans. Sustain. Energy*, vol. 8, no. 4, pp. 1658–1667, Oct. 2017.
[181] S. Dong, J. Feng, Y. Zhang, S. Tong, J. Tang, and B. Xiong, "State of charge estimation of vanadium redox flow battery based on online equivalent circuit model," in *Proc. 31st Australas. Universities Power Eng. Conf. (AUPEC)*, Sep. 2021, pp. 1–6.
[182] B. Xiong, J. Zhao, Z. Wei, and M. Skyllas-Kazacos, "Extended Kalman filter method for state of charge estimation of vanadium redox flow battery using thermal-dependent electrical model," *J. Power Sources*, vol. 262, pp. 50–61, Sep. 2014.
[183] Z. Wei, S. Meng, K. J. Tseng, T. M. Lim, B. H. Soong, and M. Skyllas-Kazacos, "An adaptive model for vanadium redox flow battery and its application for online peak power estimation," *J. Power Sources*, vol. 344, pp. 195–207, Mar. 2017.
[184] M. Pugach, S. Parsegov, E. Gryazina, and A. Bischi, "Output feedback control of electrolyte flow rate for vanadium redox flow batteries," *J. Power Sources*, vol. 455, Apr. 2020, Art. no. 227916.
[185] A. Bhattacharjee and H. Saha, "Development of an efficient thermal management system for vanadium redox flow battery under different charge-discharge conditions," *Appl. Energy*, vol. 230, pp. 1182–1192, Nov. 2018.
[186] A. Trovò, G. Marini, A. Sutto, P. Alotto, M. Giomo, F. Moro, and M. Guarnieri, "Standby thermal model of a vanadium redox flow battery stack with crossover and shunt-current effects," *Appl. Energy*, vol. 240, pp. 893–906, Apr. 2019.
[187] N. Ra and A. Bhattacharjee, "Prediction of vanadium redox flow battery storage system power loss under different operating conditions: Machine learning based approach," *Int. J. Energy Res.*, vol. 46, no. 15, pp. 24441–24453, Dec. 2022.
[188] Y. Li, X. Zhang, J. Bao, and M. Skyllas-Kazacos, "Control of electrolyte flow rate for the vanadium redox flow battery by gain scheduling," *J. Energy Storage*, vol. 14, pp. 125–133, Dec. 2017.
[189] B. Xiong, J. Zhao, K. J. Tseng, M. Skyllas-Kazacos, T. M. Lim, and Y. Zhang, "Thermal hydraulic behavior and efficiency analysis of an all-vanadium redox flow battery," *J. Power Sources*, vol. 242, pp. 314–324, Nov. 2013.
[190] H. Cao, X. Zhu, H. Shen, and M. Shao, "A neural network based method for real-time measurement of capacity and SOC of vanadium redox flow battery," in *Proc. ASME 13th Int. Conf. Fuel Cell Sci., Eng. Technol.*, Jun. 2015, Art. no. V001T02A001.
[191] B. Xiong, J. Tang, Y. Li, C. Xie, Z. Wang, X. Zhang, and H. B. Gooi, "Design of a two-stage control strategy of vanadium redox flow battery energy storage systems for grid application," *IEEE Trans. Sustain. Energy*, vol. 13, no. 4, pp. 2079–2091, Oct. 2022.
[192] L. Barelli, G. Bidini, D.-A. Ciupageanu, M. De Giorgi, F. Gallorini, C. Mazzoni, P. A. Ottaviano, and D. Pelosi, "Electrical performance analysis of an innovative vanadium redox flow battery stack for enhanced power density applications," in *Proc. IEEE Madrid PowerTech*, Jun. 2021, pp. 1–6.
[193] A. Trovo, F. Picano, and M. Guarnieri, "Comparison of energy losses in a 9 kW vanadium redox flow battery," *J. Power Sources*, vol. 440, Nov. 2019, Art. no. 227144.
[194] Y.-S. Chen, S.-Y. Ho, H.-W. Chou, and H.-J. Wei, "Modeling the effect of shunt current on the charge transfer efficiency of an all-vanadium redox flow battery," *J. Power Sources*, vol. 390, pp. 168–175, Jun. 2018.
[195] F. Xing, H. Zhang, and X. Ma, "Shunt current loss of the vanadium redox flow battery," *J. Power Sources*, vol. 196, no. 24, pp. 10753–10757, 2011.
[196] A. Tang, J. McCann, J. Bao, and M. Skyllas-Kazacos, "Investigation of the effect of shunt current on battery efficiency and stack temperature in vanadium redox flow battery," *J. Power Sources*, vol. 242, pp. 349–356, Nov. 2013.
[197] A. Clemente and R. Costa-Castelló, "Redox flow batteries: A literature review oriented to automatic control," *Energies*, vol. 13, no. 17, p. 4514, Sep. 2020.
[198] H.-W. Chou, F.-Z. Chang, H.-J. Wei, B. Singh, A. Arpornwichanop, P. Jienkulsawad, Y.-S. Chou, and Y.-S. Chen, "Locating shunt currents in a multistack system of all-vanadium redox flow batteries," *ACS Sustain. Chem. Eng.*, vol. 9, no. 12, pp. 4648–4659, Mar. 2021.
[199] S. Maurya, P. T. Nguyen, Y. S. Kim, Q. Kang, and R. Mukundan, "Effect of flow field geometry on operating current density, capacity and performance of vanadium redox flow battery," *J. Power Sources*, vol. 404, pp. 20–27, Nov. 2018.
[200] B. Xiong, Y. Yang, J. Tang, Y. Li, Z. Wei, Y. Su, and Q. Zhang, "An enhanced equivalent circuit model of vanadium redox flow battery energy storage systems considering thermal effects," *IEEE Access*, vol. 7, pp. 162297–162308, 2019.
[201] A. Tang, J. Bao, and M. Skyllas-Kazacos, "Studies on pressure losses and flow rate optimization in vanadium redox flow battery," *J. Power Sources*, vol. 248, pp. 154–162, Feb. 2014.
[202] J. Fu, M. Zheng, X. Wang, J. Sun, and T. Wang, "Flow-rate optimization and economic analysis of vanadium redox flow batteries in a load-shifting application," *J. Energy Eng.*, vol. 143, no. 6, Dec. 2017, Art. no. 04017064.
[203] T. Jirabovornwisut, S. Kheawhom, Y.-S. Chen, and A. Arpornwichanop, "Optimal operational strategy for a vanadium redox flow battery," *Comput. Chem. Eng.*, vol. 136, May 2020, Art. no. 106805.
[204] R. Badrinarayanan, K. J. Tseng, B. H. Soong, and Z. Wei, "Modelling and control of vanadium redox flow battery for profile based charging applications," *Energy*, vol. 141, pp. 1479–1488, Dec. 2017.
[205] M. Moore, R. Counce, J. Watson, and T. Zawodzinski, "A comparison of the capital costs of a vanadium redox-flow battery and a regenerative hydrogen-vanadium fuel cell," *J. Adv. Chem. Eng.*, vol. 5, no. 4, 2015, Art. no. 1000140.
[206] J. Noack, L. Wietschel, N. Roznyatovskaya, K. Pinkwart, and J. Tübke, "Techno-economic modeling and analysis of redox flow battery systems," *Energies*, vol. 9, no. 8, p. 627, Aug. 2016.
[207] R. Gundlapalli, S. Kumar, and S. Jayanti, "Stack design considerations for vanadium redox flow battery," *INAE Lett.*, vol. 3, no. 3, pp. 149–157, Sep. 2018.
[208] F. Moro, A. Trovò, S. Bortolin, D. D. Col, and M. Guarnieri, "An alternative low-loss stack topology for vanadium redox flow battery: Comparative assessment," *J. Power Sources*, vol. 340, pp. 229–241, Feb. 2017.
[209] F. T. Wandschneider, S. Röhm, P. Fischer, K. Pinkwart, J. Tübke, and H. Nirschl, "A multi-stack simulation of shunt currents in vanadium redox flow batteries," *J. Power Sources*, vol. 261, pp. 64–74, Sep. 2014.

[210] H. Chen, S. Wang, H. Gao, X. Feng, C. Yan, and A. Tang, "Analysis and optimization of module layout for multi-stack vanadium flow battery module," *J. Power Sources*, vol. 427, pp. 154–164, Jul. 2019.
[211] Z. Huang and A. Mu, "Research and analysis of performance improvement of vanadium redox flow battery in microgrid: A technology review," *Int. J. Energy Res.*, vol. 45, no. 10, pp. 14170–14193, Aug. 2021.
[212] M. Skyllas-Kazacos, G. Kazacos, G. Poon, and H. Verseema, "Recent advances with UNSW vanadium-based redox flow batteries," *Int. J. Energy Res.*, vol. 34, no. 2, pp. 182–189, Feb. 2010.
[213] A. Belderbos, E. Delarue, K. Kessels, and W. D'haeseleer, "The levelized cost of storage critically analyzed and its intricacies clearly explained," in *Proc. KU Leuven (Univ. Leuven) TME Working PAPER-Energy Environ.*, 2016, pp. 1–28.
[214] O. Schmidt, S. Melchior, A. Hawkes, and I. Staffell, "Projecting the future levelized cost of electricity storage technologies," *Joule*, vol. 3, no. 1, pp. 81–100, Jan. 2019.
[215] R. M. Darling, "Techno-economic analyses of several redox flow batteries using levelized cost of energy storage," *Current Opinion Chem. Eng.*, vol. 37, Sep. 2022, Art. no. 100855.
[216] K. E. Rodby, T. J. Carney, Y. A. Gandomi, J. L. Barton, R. M. Darling, and F. R. Brushett, "Assessing the levelized cost of vanadium redox flow batteries with capacity fade and rebalancing," *J. Power Sources*, vol. 460, Jun. 2020, Art. no. 227958.
[217] M.-J. Li, W. Zhao, X. Chen, and W.-Q. Tao, "Economic analysis of a new class of vanadium redox-flow battery for medium- and large-scale energy storage in commercial applications with renewable energy," *Appl. Thermal Eng.*, vol. 114, pp. 802–814, Mar. 2017.
[218] F. Gu and H. Chen, "Modelling and control of vanadium redox flow battery for smoothing wind power fluctuation," *IET Renew. Power Gener.*, vol. 15, no. 15, pp. 3552–3563, Nov. 2021.
[219] A. Trovo, V. D. Noto, J. E. Mengou, C. Gamabaro, and M. Guarnieri, "Fast response of kW-class vanadium redox flow batteries," *IEEE Trans. Sustain. Energy*, vol. 12, no. 4, pp. 2413–2422, Oct. 2021.
[220] R. P. Bataglioli, R. M. Monaro, D. V. Coury, and O. Anaya-Lara, "Wind generator protection with ESSs considering grid connected and island mode operations," *Int. J. Electr. Power Energy Syst.*, vol. 126, Mar. 2021, Art. no. 106594.

ANUOLUWAPO ALUKO (Member, IEEE) received the B.Eng. degree (Hons.) in electrical and electronics engineering from The Federal University of Technology Akure, Nigeria, in 2014, the M.Eng. degree in electrical power engineering from the Durban University of Technology, Durban, South Africa, in 2018, and the Ph.D. degree in electrical engineering from the University of KwaZulu-Natal, South Africa, in 2021. He is currently a Postdoctoral Associate with the Power Research Laboratory, University of Calgary. His research interests include microgrids, power system stability and control, and large-scale renewable energy integration.

ANDY KNIGHT (Senior Member, IEEE) received the B.A. and Ph.D. degrees from the University of Cambridge, in 1994 and 1998, respectively.

He is currently a Professor and the Head of the Department of Electrical and Software Engineering, University of Calgary. His research interests include energy conversion and clean and efficient energy utilization. He was a recipient of the IEEE PES Prize Paper Award and three Best Paper Awards from IEEE IAS. He was the IAS Publications Chair, the Steering Committee Chair of the IEEE ECCE and IEEE IEMDC, and the Chair of the IEEE Smart Grid Research and Development Committee. He is also the President of the IEEE IAS. He is also a Professional Engineer registered in the Province of Alberta, Canada.